Fall 2011

Effect of Reworking and Bioturbation on Sedimentary Reactive Iron Within a Microtidal Estuary

Amy Kathleen Pitts
Old Dominion University

EFFECT OF PHYSICAL REWORKING AND BIOTURBATION ON SEDIMENTARY REACTIVE IRON WITHIN A MICROTIDAL ESTUARY

by

Amy Kathleen Pitts
B.A. May 1999, University of North Carolina

A Thesis Submitted to the Faculty of
Old Dominion University in Partial Fulfillment of the
Requirements for the Degree of

MASTER OF SCIENCE

OCEAN AND EARTH SCIENCES

OLD DOMINION UNIVERSITY
December 2011

Approved by:

David J. Burdige (Director)

Desmond C. Cook (Member)

Peter N. Sedwick (Member)

ABSTRACT

EFFECT OF PHYSICAL REWORKING AND BIOTURBATION ON SEDIMENTARY REACTIVE IRON WITHIN A MICROTIDAL ESTUARY

Amy Kathleen Pitts
Old Dominion University, 2011
Director: Dr. David J. Burdige

Mixed redox conditions in sediments due to physical reworking may allow for enhanced remineralization of refractory organic matter due to Fe(III) redox cycling. In part this may occur because easily reducible iron oxides can be used by heterotrophic bacteria to remineralize the organic carbon. This phenomena has been observed in bioturbated sediments and in areas where physical factors (such as strong bottom currents) constantly rework the sediments. To specifically determine the effects of physical reworking and bioturbation on concentrations of easily reducible iron oxides, reactive iron concentrations were measured in surface sediments taken from two contrasting sites in the York River, a Chesapeake Bay tributary. Box core samples were collected between March 2007 and December 2007. Operationally defined iron fractions as well as total iron concentrations were measured using chemical extraction methods. Concentrations of easily reducible iron oxides and total iron at the site experiencing physical reworking were higher than those at the bioturbated site. A selection of sediments were also further analyzed using X-ray diffraction (XRD) and Mössbauer Spectroscopy (MS). Initial XRD analysis did not indicate the presence of iron oxides due to possible interference by the high concentrations of major mineral species such as quartz, or possibly due to nanophase Fe minerals. 300 K and 77 K MS analysis allowed for the determination of Fe(II) and Fe(III) fractions in the samples. Specific iron minerals were not discerned at these temperatures. The Fe(II) and Fe(III) results obtained using XRD combined with the results obtained through chemical extraction did not agree with the amount of Fe(III) obtained using MS. Total iron calculated using XRD analysis was within 1-2% (absolute percentage) of total iron obtained by ashing sediments and extracting Fe chemically for the majority of sites compared. However, XRD determined concentrations of easily reducible iron oxides were not consistent with the results obtained through chemical extraction.

ACKNOWLEDGMENTS

This thesis would not have been possible without the support, encouragement, and enthusiasm of my advisor, Dr. David Burdige. He challenged me and assisted me through this program. As a member of David's lab I was afforded the opportunity to participate in a research cruise, present at a conference, and develop a true appreciation of different components of scientific research.

I would also like to thank my committee members, Dr. Desmond Cook and Dr. Peter Sedwick, for their support. Thanks to Dr. Cook's willingness to allow us to conduct research in his lab we were able to utilize Mössbauer Spectroscopy to get a better handle on the composition of the York River Sediments.

My graduate school student peers were also very supportive. I would like to thank Renee Reilly for her amazing assistance with statistical analysis, and Wes Myers for helping me with XRD analysis, and for introducing me to RockJock.

I would like to thank my immediate and extended family for keeping me grounded during graduate school.

Finally, my deepest gratitude goes to my parents for their moral support and constant encouragement.

TABLE OF CONTENTS

LIST OF TABLES v

LIST OF FIGURES vi

Chapter

1. INTRODUCTION 1
    1.1. REGIONAL SETTING 5

2. MATERIALS AND METHODS 10
    2.1. SAMPLE COLLECTION 10
    2.2. IRON EXTRACTION PROCEDURE 10
    2.3. MÖSSBAUER SPECTROSCOPY AND X-RAY DIFFRACTION ANALYSIS 12

3. RESULTS 14
    3.1. CHEMICAL EXTRACTION RESULTS 14
    3.2. X-RAY DIFFRACTION ANALYSIS 26
    3.3. MÖSSBAUER SPECTROSCOPY 27

4. DISCUSSION 35
    4.1. IRON OXIDES AT CLAY BANKS CHANNEL AND GLOUCESTER POINT 35
    4.2. ANALYTICALTECHNIQUES 40

5. CONCLUSIONS 44

REFERENCES 46

VITA 52

LIST OF TABLES

Table Page

1. Average SSA Measurements from Palomo and Canuel (2010). 7

2. Iron Fraction Abbreviations. 10

3. Extraction efficiencies for extractable iron oxides using five step extraction method. 16

4. Concentrations of Highly Reactive, Reactive, and Total Fe (wt% Fe). 18

5. Concentrations of adsorbed Fe(II), Carbonate Fe, Magnetite, and Poorly Reactive Fe (wt% Fe). 20

6. Pyrite extraction results (wt% Fe). 21

7. Undefined Iron, representing the difference between the total Fe determined though ashing and the amount of Fe extracted through the five-step process, Fe(II) and pyrite extractions (when available). 24

8. Extraction efficiencies and undefined Fe, December CBC. 25

9. XRD and Chemical Extractions: March CBC with and without corundum standard addition (wt% Fe). 29

10. XRD and Chemical Extractions: August CBC and June GP, without corundum standard addition (wt% Fe). 30

11. MS Comparison of Fe(II) and Fe(III). 31

12. Comparison of Fe(II) and Fe(III), as derived through XRD and MS. 31

13. Comparison of Chesapeake Bay Tributary Sediment Surface Area to wt%. 38

14. Comparison of Sediment Iron Concentrations Measured in Tropical and Temperate Climates. 39

15. Fe(II):Fe(III) Analysis of CBC and GP Sediments. 42

LIST OF FIGURES

Figure Page

1. Map of the Chesapeake Bay and the York River. 5

2. York River sampling sites, Clay Bank Channel and Gloucester Point. 6

3. Time series of water column physical parameters measured at Clay Bank and Gloucester Point. 9

4. CBC and GP Extraction Results. 15

5. Average concentration of extractable Fe as a percent of total Fe for each site during the study period 16

6. CBC and GP Extraction results, as a percent of Fe_T. 17

7. Fe Extraction Results, normalized to sediment surface area. 19

8. CBC and GP extraction results, as a percent of Fe_T. 21

9. Average of reactive Fe, undefined Fe and remaining reactive Fe at (a) CBC and (b)GP. 22

10. Mössbauer results, March CBC. 32

11. Mössbauer results, December GP. 33

12. Mössbauer results, March GP and August CBC. 34

13. Potential pathways for Fe at physically reworked site. 35

CHAPTER 1

INTRODUCTION

Iron, the fourth most abundant element in Earth's crust (Taylor and Konhauser, 2011), is among a unique group of elements that experience redox cycling in surface environments (Poulton, 2003) [1]. Iron(III) is reduced in natural environments through biotic and abiotic processes, and may act as an electron acceptor for heterotrophic bacteria oxidizing organic matter within the sediments, potentially increasing the amount of carbon remineralized at a given site. Iron(III) minerals such as ferrihydrite, lepidocrocite, goethite, and hematite will react with sulfide when present, and in many environments Fe(III) minerals are eventually reduced and transformed to pyrite (Berner, 1970; Raiswell, 2006; Canfield, 1989; Kostka and Luther III, 1994). Minerals react with sulfide on different time scales; for example, minerals containing easily reducible iron, such as ferrihydrite and lepidocrocite, can be reduced quickly, i.e. within hours (Canfield et al., 1992), while iron present in silicates reacts on time scales as long as 10^5-10^6 years (Poulton, 2003; Poulton and Raiswell, 2005). Typically sulfide production via sulfate reduction occurs in anoxic environments (Raiswell, 2006), and the presence of oxygen in pore waters impedes sulfate reduction and increases the likelihood iron will be oxidized and re-precipitate as an oxide phase (Balzer, 1982; Sundby et al., 1986; Canfield, 1989; Gerringa, 1990; Alongi et al., 1993). Physical reworking due to strong bottom currents, and bioturbation, caused by organisms burrowing into the sediments, can introduce oxygen into sediments, reoxidize iron sulfide minerals and buffer pore water sulfide concentrations (Canfield, 1989). Easily reducible iron adsorbed to sediments and evidence of iron redox cycling has been observed in areas of intense physical reworking such as the Gulf of Papua (Alongi et al., 1993) and the Amazon River basin (Aller and Blair, 1996).

On the Amazon basin shelf, physical reworking of sediments occurs in the upper 1-2 m of the sea floor (Aller and Blair, 1996) and iron redox cycling, not sulfate reduction, is thought to be the primary pathway for anaerobic organic matter remineralization. In the Gulf of Papua, bottom waters are well oxygenated and diffusion of oxygen into sediments was similar to that observed in temperate and tropical estuarine regions (Aller et al., 2004). Concentrations of total iron (Fe_T), highly reactive iron (Fe_{HR}), which includes the minerals ferrihydrite and lepidocrocite, and reactive iron

[1] This thesis follows the style of *Marine Chemistry*

(Fe_R), defined as hematite and goethite, were measured in Gulf of Papua sediments; high total and reactive Fe concentrations were found in the areas with the greatest physical reworking (Aller et al., 2004). Iron and manganese reduction, not sulfate reduction, were argued to be the dominant pathways for carbon remineralization in many areas of the Gulf of Papua (Aller et al., 2004).

Sediments in the Amazon delta and the Gulf of Papua experience massive physical reworking due to tides, estuarine circulation, river flow into the delta, and wind (Aller, 1998; Aller et al., 2004) and this reworking introduces oxygen into the sediments, which oxidizes metals such as Fe and Mn. Metal oxides produced in this manner presumably then act as electron acceptors in the remineralization of organic matter (Aller, 1998; Aller et al., 2004; Arzayus and Canuel, 2005). This results in the conversion of organic carbon deposited from marine and terrestrial sources into inorganic carbon via heterotrophic bacteria. In the absence of such bacteria, organic carbon is more likely to be buried in the sediment layer and preserved (Burdige, 2006). In the Amazon basin and the Gulf of Papua and other similar areas, bioturbation is an additional process in sediments that introduces O_2 to the pore waters by means other than diffusion and increases Fe and Mn redox cycling (Burdige, 2006). Although the forces driving physical reworking in an estuary are typically not as intense as those in the Amazon delta and Gulf of Papua, strong currents are present (Dellapenna et al., 2001; Schaffner et al., 2001) and increased degradation of refractory organic matter within such estuarine sediments due to high bottom-water velocity has been inferred (Arzayus and Canuel, 2005).

Solid phase iron can often be found in substantial proportions in estuarine and deltaic sediments (Raiswell, 2006). Concentrations of total iron and reactive iron found in sediments decreases in transit from rivers to the continental shelf while concentrations of non-reactive iron, including iron silicates, increases (Poulton and Raiswell, 2002). Samples from the Beulieu River in Southern England contained lepidocrocite and ferrihydrite, highly reactive iron minerals, making up 8-16% of particulate matter in the river but only 1% of particulate matter in coastal waters outside of the estuary (Poulton and Raiswell, 2002; Moore et al., 1979). In estuarine waters where saltwater meets freshwater, increasing salinity causes dissolved iron to precipitate (Boyle et al., 1977). The resulting solid iron is deposited on floodplains and in marshes and estuaries (Poulton and Raiswell, 2002). Iron deposits are also

found on the surface of fine grained sediments such as clays, which have greater sediment surface area than coarse grained materials such as sands (Poulton, 2003).

Determining whether electron acceptors such as Fe(III) may play a role in OM remineralization can begin with an analysis of OM at the study site. Palomo and Canuel (2009) analyzed sediments in the York River, a tributary of the Chesapeake Bay, for total organic carbon (TOC), total nitrogen (TN), and neutral and phospholipid linked fatty acids. Samples were taken from an area with strong physical reworking and an area with high rates of bioturbation. When the results were normalized to sediment surface area, higher concentrations of TOC and TN were observed at the bioturbated site (Palomo and Canuel, 2010). This suggests enhanced remineralization in the sediments from the site undergoing physical reworking, potentially due to increased sediment oxygen concentrations and increased sediment mixing (Palomo and Canuel, 2010). Bacterial biomass, measured by phospholipid linked fatty acids, increased after a phytoplankton bloom at the site experiencing high physical reworking, suggesting the heterotrophic bacteria responded to an increase of organic carbon. Since iron(III) can act as a terminal electron acceptor for bacteria as they remineralize organic matter, increased concentrations of easily reducible iron oxides at the site may play a role in the increased remineralization rates.

Iron's impact on organic matter degradation does not have to be mediated by biological interactions. The presence of iron(III) in physically reworked areas may allow for the abiotic degradation of organic matter. Iron(II) in high energy marine environments can become oxidized, resulting in the formation of Fenton's reagent, a strong oxidant formed by combining Iron(II) and H_2O_2 (Burdige, 2006; Hedges and Keil, 1995). The spontaneous formation of Fenton's reagent may play a significant role in the degradation of refractory organic matter, and cannot be ignored as a potential remineralization pathway at high energy oxic sites (Burdige, 2006; Walling, 1975).

In sediments from areas that experience intense redox cycling due to physical and biological processes, it is thought that ferrihydrite is the predominate iron oxide phase to precipitate in these environments via iron(II) oxidation (van der Zee et al., 2005). Standard chemical extractions identify operationally defined fractions of iron, typically iron minerals showing similar levels of reactivity, but cannot determine concentrations of specific mineral phases (Poulton and Canfield, 2005; van der Zee et al.,

2005, 2003). Sediments analyzed using x-ray diffraction (XRD) and transmission electron microscopy are unable to detect nanophase iron oxides, amorphous phases, or oxides with poor crystalline structures, due to poor reflectivity and low concentration relative to higher concentrations of more crystalline mineral phases such as quartz in the sediments (van der Zee et al., 2003, 2005).

In an attempt to overcome these limitations, and to produce a more complete picture of iron geochemistry in oxygenated sediments, van der Zee et al. (2003, 2005) used Mössbauer Spectroscopy at room temperature and 4.2 K (liquid helium temperature) to analyze sediment samples from the Mediterranean Sea and boreal forest lakes in Canada containing 'reactive' iron oxides as defined by citrate-dithionite-bicarbonate extraction. Liquid helium temperature is necessary to resolve poorly crystalline iron oxides as well as nanophase oxides (van der Zee et al., 2005), as these iron minerals only become magnetic at 4 K. Only magnetic minerals will express unique sextet signatures, allowing for mineral identification; it should be noted many iron minerals are paramagnetic at room temperature or at 77 K (Long, 1984). The Mössbauer analysis was able to differentiate Fe(III) bound to clays as well as iron oxides formed through precipitation. Analysis of these marine and lacustrine samples showed that the predominant iron oxide precipitate was nanophase goethite (van der Zee et al., 2003, 2005), a phase that was not observed in XRD results. Furthermore, the crystalline iron oxide ferrihydrite was not found in sediments analyzed through Mössbauer Spectroscopy (van der Zee et al., 2003, 2005).

This study will examine the effect of bioturbation and physical reworking of sediments on reactive iron concentrations in the York River, a tributary of the Chesapeake Bay. The organic matter in the sediments are periodically exposed to oxygen due to these processes (Canfield, 1989; Aller, 2001; McKee et al., 2004), creating an environment of alternating oxic and sub-oxic/anoxic conditions in which Fe redox reactions could be an important means of carbon remineralization.

The thesis will address the following questions:

- Does physical reworking create a significantly different environment with greater concentrations of reactive iron as compared to an area with less physical reworking but significant bioturbation?

- Can increased concentrations of reactive iron at the study sites in the York River explain the greater organic mineral remineralization observed by Palomo and Canuel (2010)?

- Will seasonal flow variation or seasonal bloom cycles significantly impact the concentrations of reactive iron in the study areas?
- What is the relationship between iron concentrations determined using chemical extraction methods versus quantitative results obtained through analysis of sediments using Mössbauer spectroscopy and X-ray diffraction?

1.1 REGIONAL SETTING

The York River is roughly 53 km long (Lin and Kuo, 2001) and begins at the confluence of the Pamunkey and Mattaponi rivers, flowing into the Chesapeake Bay at Gloucester Point (Fig. 1).

Physical reworking dominates sediments in the mid and upper reaches of the river, while bioturbation dominates sediments near the mouth of the river (Friedrichs et al., 2008). A permanent turbidity maximum exists where the three rivers converge (Fig. 2) (Schaffner et al., 2001). The middle portion of the York River has a secondary turbidity maximum zone (STM) due to tidal energy and river flow (Lin and Kuo,

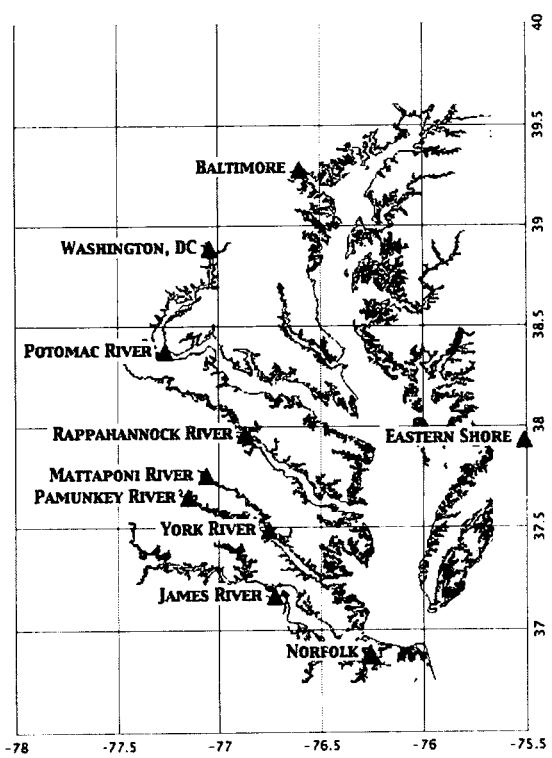

Figure 1: Map of the Chesapeake Bay and the York River.

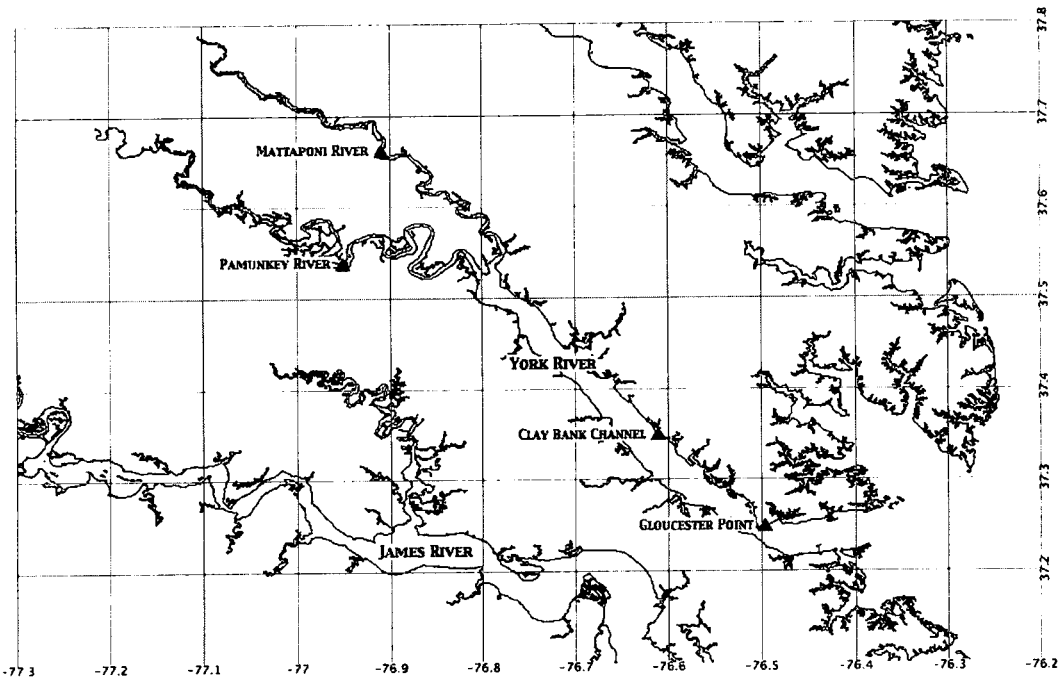

Figure 2: York River sampling sites, Clay Bank Channel and Gloucester Point.

2001). A primary and secondary channel are found at the Clay Bank Channel site (CBC) in the mid-York River. Physical reworking is responsible for a sediment mixing depth of up to 40 cm in the secondary channel and up to 110 cm in the primary channel (Dellapenna et al., 2001). The sediments found at Clay Bank are classified as silty clay (Lin and Kuo, 2001) and the sedimentation rate over the last 350 years is 0.2 cm yr^{-1} (Dellapenna et al., 1998). Average grain size is generally larger at the Gloucester Point (GP) site (Palomo and Canuel, 2010) although sediment composition at GP is similar to the silty clays seen at Clay Bank (Arzayus and Canuel, 2005). Sediment surface area (SSA), a proxy for grain size, was measured at each site when sampled by Palomo and Canuel (2010) (Table 1). SSA measurements are inversely proportional to sediment size.

As one moves down river from Clay Bank into the lower York River the average water column depth increases from 5 m to 15 m and the width of the river also increases (Dellapenna et al., 2001; Schaffner et al., 2001; Arzayus and Canuel, 2005). The tidal and fluvial energy in the lower York River is significantly less than the middle and upper York River, with bottom currents measured at 20-40 cm s^{-1}. Biological activity is responsible for sediment mixing to depths of 8 to 16 cm (Arzayus and

Table 1: Average SSA Measurements from Palomo and Canuel (2010). (m^2g^{-1})

	GP	CBC
March	16.2 ± 0.5	23.4 ± 0.2
April	17.4 ± 0.1	23.7 ± 0.9
May	19.3 ± 2.1	20.3 ± 0.2
June	14.0 ± 0.1	24.2 ± 0.1
August	22.2 ± 0.5	21.8 ± 0.2
October	18.8 ± 0.7	23.0 ± 0.4

Canuel, 2005) in the lower York River and biological reworking of the sediments at GP is similar to that observed in the Severn River, Bay of Fundy, and areas of the Amazon Shelf (Schaffner et al., 2001).

The spring tidal range at Clay Bank is more than 2m and the site is considered to be a microtidal environment (Nichols and Biggs, 1985; Schaffner et al., 2001). The bottom currents resulting from tidal and fluvial energy range from 60-70 cm s^{-1} and there is little bioturbation (Arzayus and Canuel, 2005). Erosion of the Clay Bank bed is seen during periods of increased discharge, such as in the spring (Friedrichs et al., 2008).

As one moves down river from Clay Bank into the lower York River, the average water column depth increases from 5 m to 15 m and the width of the river also increases (Dellapenna et al., 2001; Schaffner et al., 2001; Arzayus and Canuel, 2005). The tidal and fluvial energy in the lower York River is significantly less than the middle and upper York River, with bottom currents measured at 20-40 cm s^{-1}. Biological activity is responsible for sediment mixing to depths of 8 to 16 cm (Arzayus and Canuel, 2005) in the lower York River and biological reworking of the sediments at GP is similar to that observed in the Severn River, Bay of Fundy, and areas of the Amazon Shelf (Schaffner et al., 2001).

Each spring large volumes of freshwater flow from the Pamunkey and Mattaponi rivers into the York River and the Chesapeake Bay, and each summer river discharge decreases significantly (Palomo and Canuel, 2010). As a result, tidal intrusion into the York River increases in the summer months (Palomo and Canuel, 2010) increasing water column salinity in the STM (Virginia Estuarine and Coastal Observing System

(VECOS) database, 2007) (Fig. 3a). Water temperature also increases during the summer months (Fig. 3b) and levels of bottom water dissolved oxygen decrease from 80-90% saturation in May to 60-70% saturation in October, due to benthic organic matter remineralization (Palomo and Canuel, 2010). Water column turbidity (Fig. 3d) reaches a maximum at Clay Bank due to increased river discharge in April, and again in July. CB turbidity decreases in June when GP turbidity is at its maximum. Turbidity values decrease at both locations in the late summer and continue to decrease into the fall, as river discharge decreases, slowing bottom currents (Virginia Estuarine and Coastal Observing System (VECOS) database, 2007).

Water column pH at Clay Bank decreases in May and does not return to spring levels until October. Conversely, pH at Gloucester Point remains relatively constant through the spring and summer into the fall (Virginia Estuarine and Coastal Observing System (VECOS) database, 2007) (Fig. 3c). The redox potential (Eh) at 0.75 cm depth in Gloucester Point sediments was greater than 200mV in the spring and decreased in June, increasing to about 100mV in the late summer and fall. At Clay Bank Eh in the sediments in March was 300mV, decreased to 0mV in May, and increased to levels seen in Gloucester Point sediments in June ($\sim$ 100mV), remaining at this Eh through the end of the study period (Palomo and Canuel, 2010).

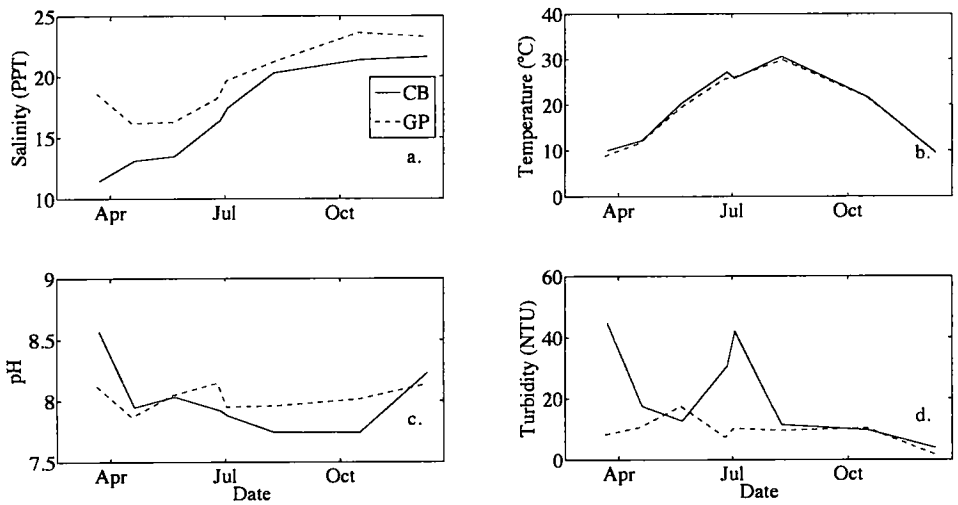

Figure 3: Time series of water column physical parameters measured at Clay Bank and Gloucester Point. Data measured by the Virginia Estuarine and Coastal Observing System (VECOS) between March and December of 2007 at a depth of 0.5m: (a) salinity, (b) temperature, (c) pH, and (d) turbidity.

CHAPTER 2

MATERIALS AND METHODS

2.1 SAMPLE COLLECTION

Samples used in this study were collected using a box corer close to slack tide from two areas, the main channel at Clay Bank (CBC) and at Gloucester Point (GP) (Fig. 2). After collection, samples were sectioned and placed into pre-combusted glass jars and frozen at -80°C. Sections from the first 3 cm of the cores were freeze dried and prepared for analysis. 100-200 mg of sediment were used for each extraction procedure.

2.2 IRON EXTRACTION PROCEDURE

The amount of highly reactive iron (Fe_{HR}), reactive iron (Fe_R), magnetite (Fe_M), carbonate iron (Fe_C), and poorly reactive iron (Fe_{PR}) found in sheet silicates were determined at each site from samples collected between March 2007 and December 2007 (Table 2). Total iron and exchangeable iron were also measured.

Table 2: Iron Fraction Abbreviations.

	Iron Fraction
Fe_T	Total Iron
Fe_{HR}	Highly Reactive Iron (e.g., Ferrihydrite and Lepidocrocite)
Fe_R	Reactive Iron (e.g., Hematite and Goethite)
Fe_M	Magnetite
Fe_{PR}	Poorly Reactive Iron (e.g., Biotite, Chlorite, Glauconite, Nontronite)
Fe_C	Iron Carbonates (e.g., Siderite and Ankerite)
Fe_U	Unreactive Iron (e.g., Iron present in clays)

A sequential extraction procedure developed by Poulton et al (2005) was employed to determine these different fractions of reactive iron. The sequence separates Fe_C

(siderite and ankerite), Fe_{HR} (ferrihydrite and lepidocrocite), Fe_R (goethite, hematite, and akaganite), Fe_M, and Fe_{PR} (biotite, chlorite, glauconite, and nontronite). Unless noted, all extractions were performed at room temperature and the samples were constantly agitated during extraction. Methods were tested for accuracy using synthetic ferrihydrite and lepidocrocite prepared according to methods described by Cornell and Schwertmann 2003. Mineral samples of goethite, hematite and magnetite were purchased from Ward's Scientific, and synthetic goethite, hematite, and magnetite samples were provided from the collection of Dr. Desmond C. Cook at Old Dominion University.

Fe_C associated iron was extracted by placing sediments into a 1M sodium acetate solution adjusted to pH 4.5 for 24 hours. To extract Fe_{HR} the samples were rinsed and next placed into an extractant of 1M hydroxylamine-HCl solution prepared in 25% acetic acid for 48 hours (Chester and Hughes, 1967; Poulton and Canfield, 2005).

Following the Fe_{HR} extraction, a two hour extraction of Fe_R was carried out in a 50g l^{-1} sodium dithionite solution at pH 4.8. The solution was buffered to pH 4.8 using a 0.35 M acetic acid/0.2 M sodium citrate solution (Mehra and Jackson, 1960; Lord III, 1980).

The fourth extraction in the sequence was performed to extract Fe_M by adding rinsed sediment to a 0.2 M ammonium oxalate/0.17 M oxalic acid solution at pH 3.2 for six hours (McKeague and Day, 1966; Phillips and Lovley, 1987). Finally, the sediments were placed into boiling 12 N HCl for 1 minute (Raiswell et al., 1994) to extract Fe_{PR}.

Total iron (Fe_T) was determined by ashing a separate aliquot of sediments at 450°C for eight hours followed by a 24 hour extraction in near boiling 6N HCl (Aller et al., 1986; Poulton and Canfield, 2005). A 1M $MgCl_2$ solution at pH 7 was used to extract Fe(II) adsorbed to the sediment surface (Tessier et al., 1979; Poulton and Canfield, 2005).

Analysis of Fe concentrations in all extracts was performed using a Perkin Elmer 330 flame atomic absorption spectrophotometer (AAS) utilizing an air acetylene gas mixture. A 1,000 ppm Fe standard solution was diluted to create standards containing 1 to 5 ppm Fe, and these standards were used to calibrate the instrument. Extracts were diluted as appropriate prior to analysis. Selected samples were also analyzed colormetrically using the ferrozine technique (Stookey, 1970) with a HP 8453E diode array UV-Vis spectrophotometer, and the results of these analyses were similar to

those obtained with the AAS. This suggests there is no matrix effect in the AA results.

Pyrite analysis was performed on a separate sediment sample using Cr(II) to reduce sulfur contained in pyrite to hydrogen sulfide, which was then determined using gas chromatography with photo-ionization detection (Cutter and Oatts, 1987). Selected samples were processed using a two step process to determine levels of AVS, as described in Cutter et al., (1987), but AVS was not detected in the sample. All remaining samples were processed using the single step pyrite extraction described above. The pyrite analysis is necessary to determine the role sulfides play, if any, in the Fe redox cycle at the sites.

2.3 MÖSSBAUER SPECTROSCOPY AND X-RAY DIFFRACTION ANALYSIS

Mössbauer Spectroscopy and x-ray diffraction were used to examine iron mineralogy and redox state. These analyses allow for a more detailed and complete analysis of the iron oxides in the sediments and for the differentiation between iron oxides and iron in clay minerals. They also offer an opportunity to compare results obtained through chemical extraction to those obtained through the non-destructive spectroscopic analysis.

XRD analyses were carried out using a PANalytical X'Pert Pro equipped with an X'celerator Detector. The instrument utilizes Co radiation at a wavelength of 1.7902 Å and voltage and current settings were 45 kV and 40 mA. All samples were scanned from 10° to 150°, at 0.02 steps per second. The March CBC sample was also scanned from 5° to 65° at 0.02 steps per second, with an added corundum standard. The XRD analysis using Rock Jock software from the USGS was used to quantify minerals and clays in the sediments (Eberl, 2003). The Rock Jock software returns normalized weight percentages of each component it detects in the sample, integrating the area under mineral peaks to estimate the amount of each mineral or clay identified (Eberl, 2003).

Transmission Mössbauer spectroscopy was performed at 300 K (room temperature) using a Wissel laser calibrated transducer. Low temperature transmission Mössbauer spectroscopy was performed at 77 K using a Janis 8DT Varitemp cryostat using a Wissel transducer in horizontal geometry. Both transducers were mounted on floating optical tables, and spectra were fit to existing standards using Recoil

software (Lagarec and Rancourt, 1998). This configuration has been used to analyze iron oxide formation on structural steel to determine the presence of protective and non-protective coatings (Cook, 2005; Oh et al., 1998), and to examine iron oxide formation in marine environments, specifically corrosion magnetite which formed on the turret of USS Monitor while submerged off the coast of North Carolina (Cook and Peterson, 2005).

Sediments were prepared for Mössbauer analysis by adding boron nitride (BN) to the sample and tablets were pressed using brass rings (Lewis and McConchie, 1994). BN is a low density powder that can be pressed to solid pellets, encompassing the iron compounds to be studied. Room temperature analysis (300 K) was performed on the samples, followed by a low temperature analysis (77 K). A third analysis at 4 K was not performed. Analyses were performed at the different temperatures in an attempt to distinguish nanophase and crystalline iron oxides that are magnetized at low temperatures (van der Zee et al., 2005), and the resulting spectra was analyzed using Lorentzian least-squares fitting, similar to the methods described in Drodt et al 1997 and König et al., 1997, 1999. Results from chemical extraction, MS, and XRD were compared to examine Fe speciation, with each technique providing certain cross checks on the other methods.

CHAPTER 3

RESULTS

3.1 CHEMICAL EXTRACTION RESULTS

Chemical extraction methods were first tested using synthetic and natural iron minerals. The results are summarized in Table 3. Difficulties were encountered when extracting defined iron minerals from natural samples, and the extractions were repeated using synthetic minerals. In the case of goethite, hematite, and magnetite, the extraction efficiency was significantly higher when using synthetic minerals. However, the synthetic hematite extraction efficiency never exceeded 52%, possibly due to difficulties observed when extracting aged hematite (Schwertmann and Murad, 1990). The aging of hematite also explains the difficulty extracting iron from the mineral hematite sample. The lepidocrocite extraction efficiency was just below 75% (84% when normalized to the amount of total iron extracted using an aliquot of synthetic lepidocrocite) and it is suspected that impurities were present in the synthesized phase which led to low recovery both when ashing the sample to determine total Fe in the samples and during the hydroxlamine-HCl extraction. To examine mineral purity, the synthetic ferrihydite was analyzed using XRD. The resulting pattern matched that of 2-line ferrihydrite and no other peaks were observed in the sample.

Results from York River sediment extractions showed elevated concentrations of iron at the Clay Bank Channel site as compared to the Gloucester Point site (Fig. 4, Tables 4 and 5). Fe_{HR}, Fe_R, and Fe_C concentrations were higher in CBC samples than GP samples, while, with the exception of the month of December, pyrite levels were always higher at GP than CBC (Tables 4, 5, and 6, Fig. 5). Further, the average pyrite concentration, expressed as a percentage of total iron, exceeded the average amount of Fe_{HR} and Fe_R at GP (Fig. 5).

Iron(II) adsorbed to sediments, Fe_M and Fe_{PR} concentrations were of minor importance at both sites (Table 5, Fig. 5), and similar levels were often observed at the two sites. Fe_M concentrations were much lower at each site compared to Fe_{HR} and Fe_R (Tables 4 and 5). Repeated measures ANOVA tests performed for each stage of the extraction sequence indicated that iron concentrations at the two sites were significantly different from each other over the time frame studied (Fig. 4 and Fig. 6).

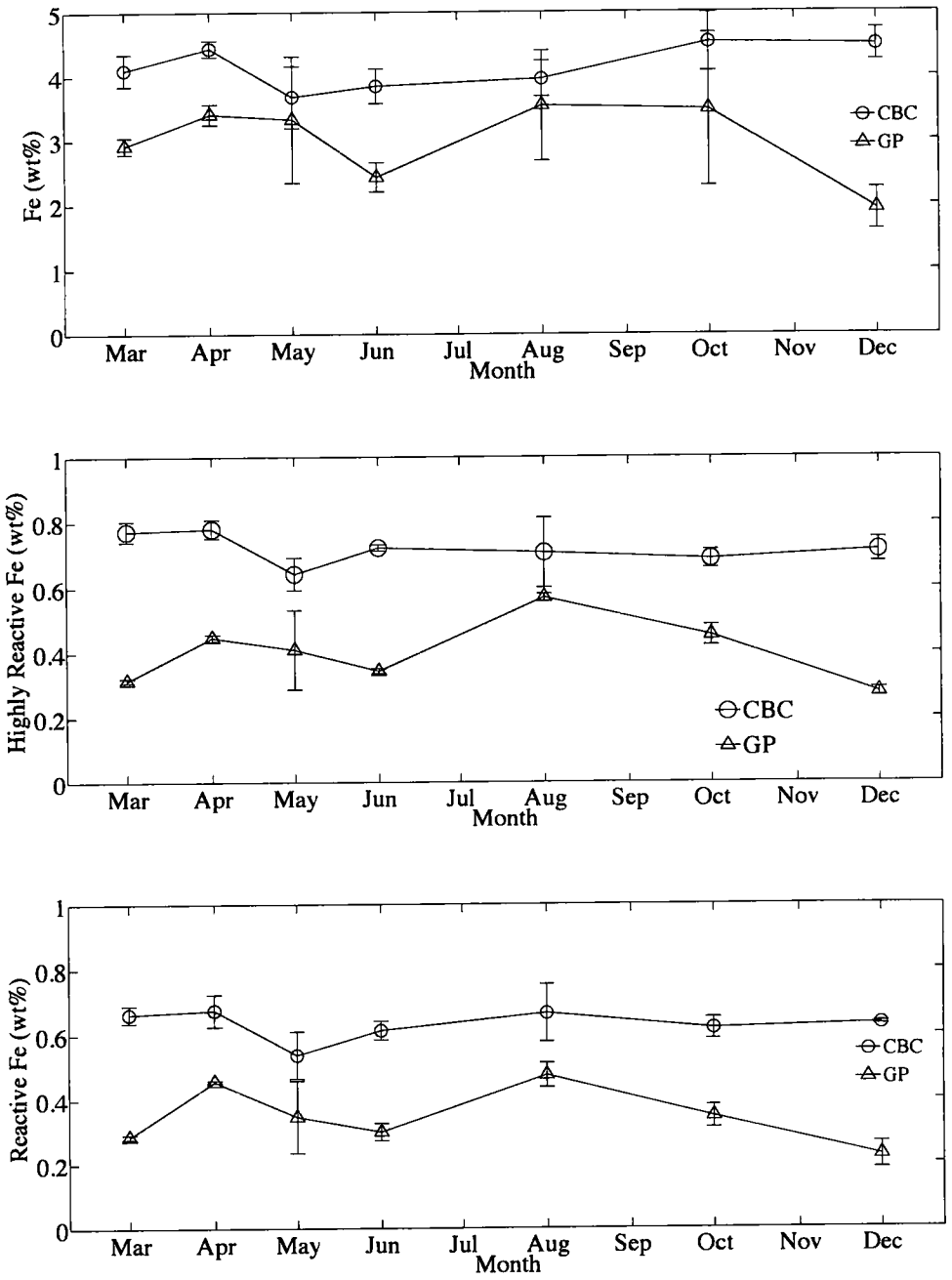

Figure 4: CBC and GP Extraction results. (a) Total Fe, (b) Highly Reactive Fe (Ferrihydrite and Lepidocrocite), (c) Reactive Fe (Hematite and Goethite).

Table 3: Extraction efficiencies for extractable iron oxides using five step extraction method. The normalization calculation involved dividing the iron extracted from the lepidocrocite sample using hydroxlamine HCL by the total iron recovered from a second sample via the ashing method. Ferrihydrite and lepidocrocite were extracted using hydroxylamine-HCl solution. Goethite and hematite were extracted using a sodium dithionite-sodium citrate solution, and magnetite was extracted using an ammonium oxalate/oxalic acid solution.

Iron Oxide	Total Fe	Fe extracted (synthetic)	Fe extracted (mineral)	Fe Extracted (Poulton et al., 2005) (Synthetic)
Ferrihydrite[a]	102 ± 4.4%	103 ± 4.4%	*n/a*	99%
Ferrihydrite[b]	102 ± 4.4%	3.3 ± 0.6%	*n/a*	99%
Lepidocrocite	89 ± 4.7%	84 ± 4.7% (normalized)	*n/a*	99%
Goethite	120 ± 5.0%	90 ± 3.6%	44 ± 3.6%	100%
Hematite	99 ± 10.2%	52 ± 1.7%	6 ± 6.1%	94%
Magnetite[c]	128 ± 19.9%	96 ± 4.3%	21 ± 7.8%	100%
Magnetite[b]	128 ± 4.4%	0.3 ± 0.04%	21 ± 7.8%	100%

[a] Extraction performed in Hydroxylamine-HCl solution.
[b] Extraction performed in pH 4.5 sodium acetate solution
[c] Extraction performed in ammonium oxalate/oxalic acid solution

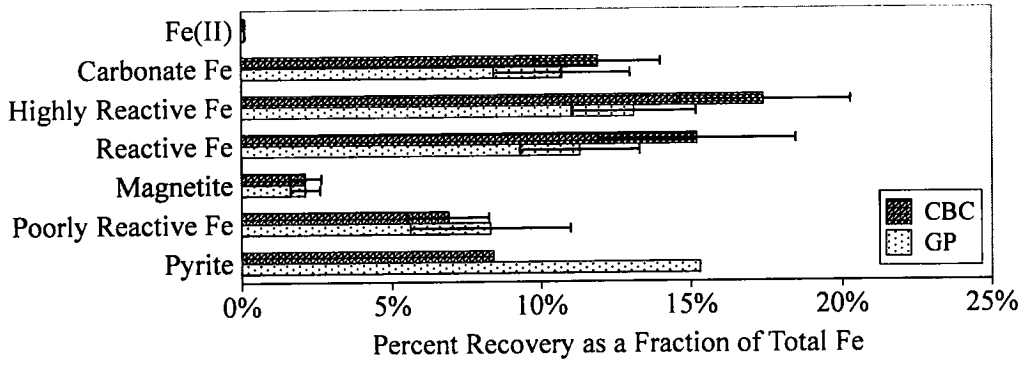

Figure 5: Average concentration of extractable Fe as a percent of total Fe for each site during the study period. Error bars represent standard deviation.

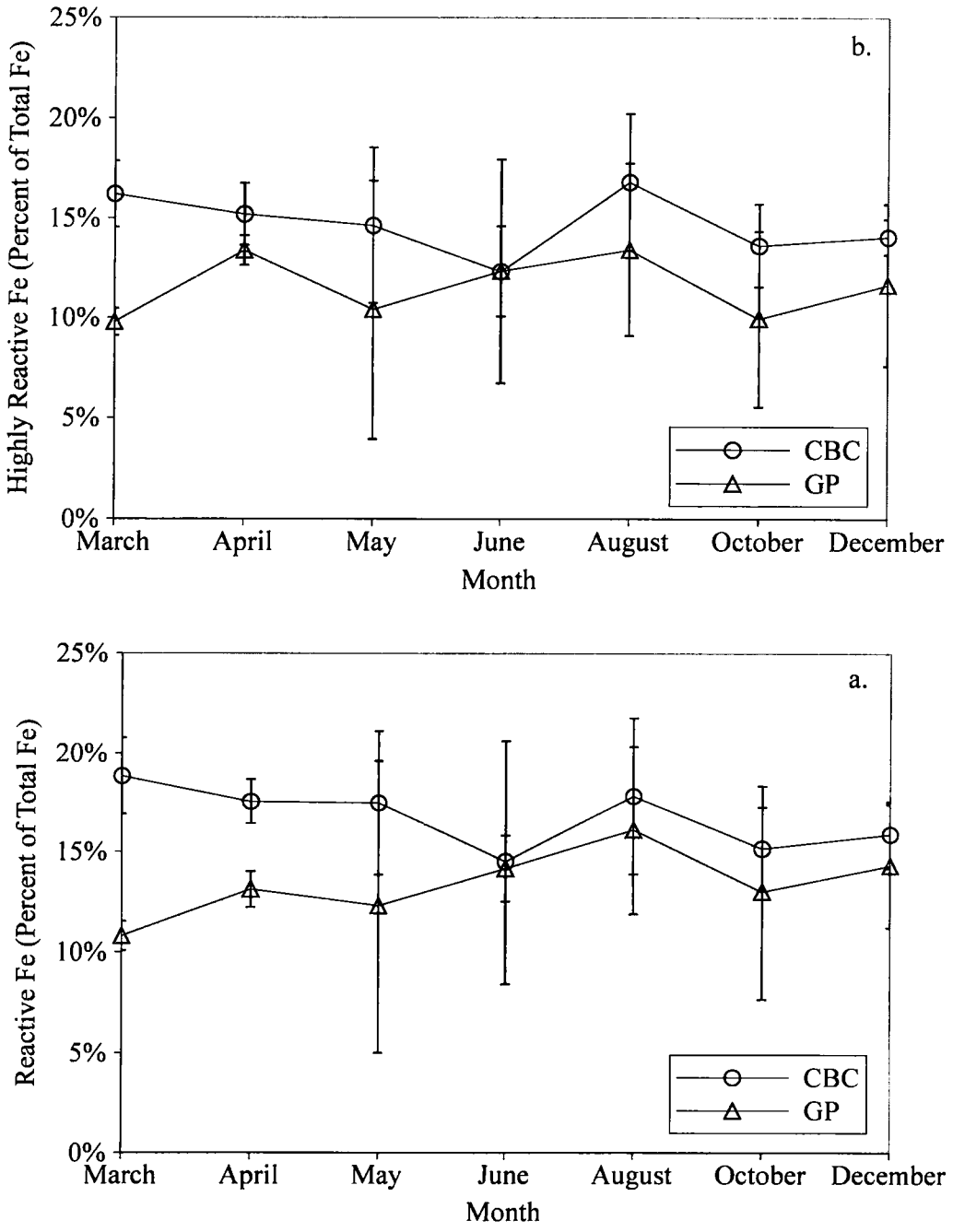

Figure 6: CBC and GP Extraction results, as a percent of Fe_T. (a) Highly Reactive Fe (Ferrihydrite and Lepidocrocite), (b) Reactive Fe (Hematite and Goethite).

Table 4: Concentrations of Highly Reactive, Reactive, and Total Fe (wt% Fe).

	Highly Reactive Fe		Reactive Fe		Total Fe	
Month	GP	CBC	GP	CBC	GP	CBC
March	0.3 ± 0.01	0.8 ± 0.03	0.3 ± 0.01	0.7 ± 0.03	3.5 ± 0.1	4.1 ± 0.3
April	0.4 ± 0.01	0.8 ± 0.03	0.5 ± 0.004	0.7 ± 0.05	3.4 ± 0.2	4.4 ± 0.1
May	0.4 ± 0.1	0.6 ± 0.05	0.3 ± 0.1	0.5 ± 0.1	3.3 ± 1.0	3.7 ± 0.5
June	0.3 ± 0.01	0.7 ± 0.01	0.3 ± 0.03	0.6 ± 0.03	2.4 ± 0.2	3.9 ± 0.3
August	0.6 ± 0.01	0.7 ± 0.1	0.5 ± 0.04	0.7 ± 0.1	3.5 ± 0.9	4.0 ± 0.3
October	0.5 ± 0.03	0.7 ± 0.03	0.3 ± 0.04	0.6 ± 0.03	3.5 ± 1.2	4.5 ± 0.5
December	0.3 ± 0.01	0.7 ± 0.04	0.2 ± 0.04	0.6 ± 0.005	1.9 ± 0.3	4.5 ± 0.2

When iron concentrations were normalized using sediment surface area data from Palomo and Canuel (2010) (Fig. 7) to examine potential relationships between grain size and iron concentrations, no significant differences in total iron were observed (Paired T-test, p=0.662), although significant differences were observed in highly reactive and reactive iron concentrations (p=0.002 and p=0.003).

The ratio of Eh to pH can be used to determine the thermodynamically stable iron species formed in sediments based on the thermodynamic database created by the Lawrence Livermore National Laboratory (LLNL) and compiled in the Atlas of Eh-pH diagrams (Takeno, 2005). In reducing marine environments, magnetite is the predominant phase, while in oxidizing environments hematite is the predominant phase (Cornell and Schwertmann, 2003). In both York River settings the predominant iron phase predicted using the Eh data collected by Palomo and Canuel (2010) and pH data available in the VECOS database (Virginia Estuarine and Coastal Observing System (VECOS) database, 2007) is hematite, but Fe_R, the extraction group which contains hematite (Table 2), was not the primary reservoir of iron in the extractions (Fig. 5). This difference between the extraction data and the thermodynamic calculations may be due to the fact that the thermodynamic data does not consider other factors affecting iron oxide stability such as sediment surface area and resulting surface energy or uncertainty in Eh measurements (Cornell and Schwertmann, 2003).

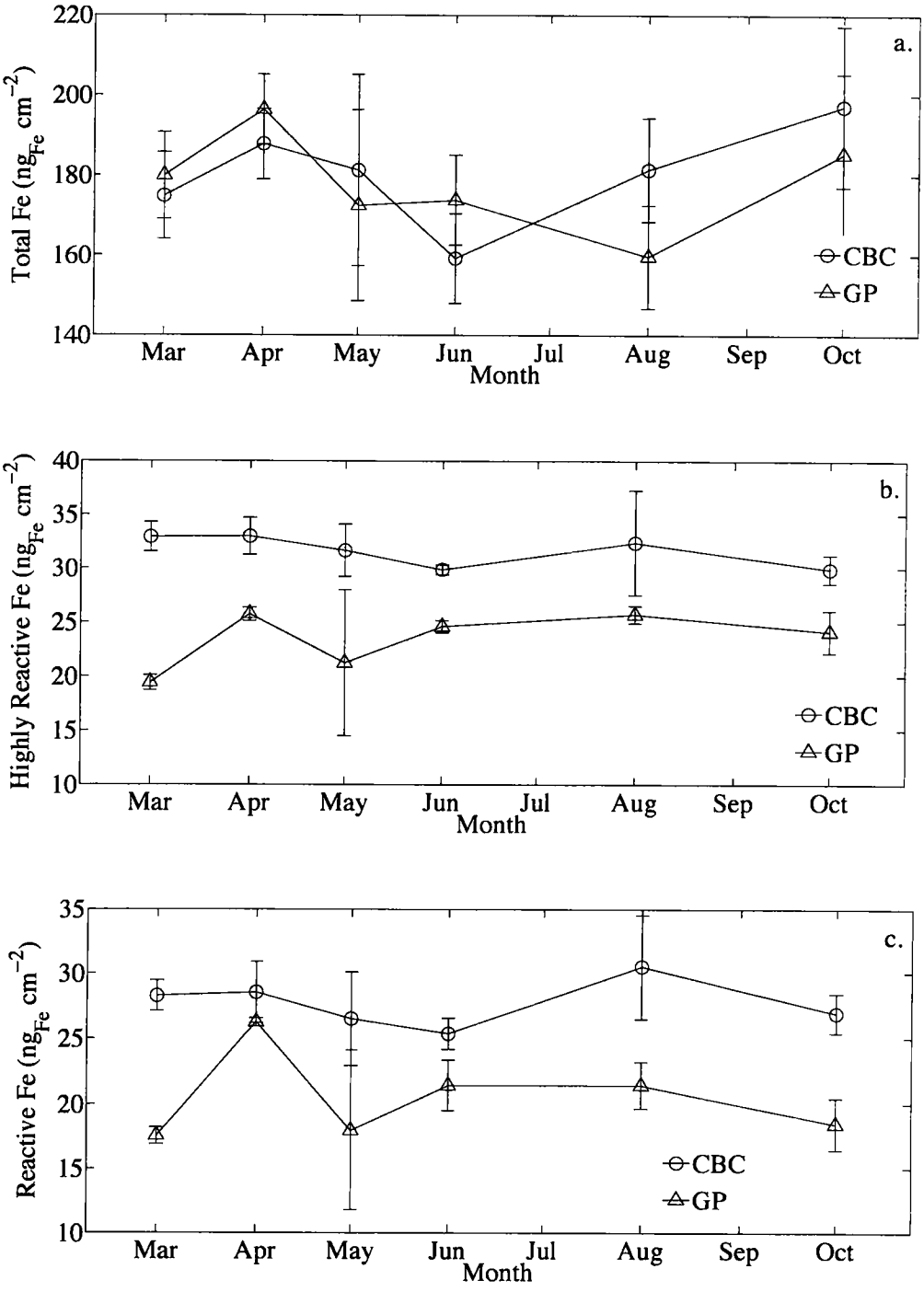

Figure 7: CBC and GP Extraction results, normalized to sediment surface area. (a) Total Fe, (b) Highly Reactive Fe (Ferrihydrite and Lepidocrocite), (c) Reactive Fe (Hematite and Goethite).

Table 5: Concentrations of adsorbed Fe(II), Carbonate Fe, Magnetite, and Poorly Reactive Fe (wt% Fe).

	Fe(II)		Carbonate Fe	
Month	GP	CBC	GP	CBC
March	0.003 ± 0.002	0.003 ± 0.001	0.323 ± 0.005	0.594 ± 0.022
April	0.002 ± 0.00003	0.002 ± 0.004	0.350 ±0.073	-
May	0.002 ± 0.001	0.003 ± 0.001	0.250 ± 0.031	0.470 ± 0.039
June	0.002 ± 0.001	0.005 ± 0.001	0.250 ± 0.031	0.450 ± 0.027
August	0.003 ± 0.002	-	0.401 ± 0.071	0.430 ± 0.009
October	0.003 ± 0.001	0.002 ± 0.0003	0.341 ± 0.004	0.447 ± 0.027
December	0.003 ± 0.001	0.005 ± 0.004	0.287 ± 0.037	0.520 ± 0.016

	Magnetite		Remaining Reactive Fe	
Month	GP	CBC	GP	CBC
March	0.058 ± 0.001	0.084 ± 0.007	0.292 ± 0.010	0.210 ± 0.020
April	0.074 ± 0.004	0.078 ± 0.002	0.224 ± 0.008	0.345 ± 0.017
May	0.062 ± 0.037	0.065 ± 0.012	0.255 ± 0.117	0.291 ± 0.013
June	0.052 ± 0.016	0.103 ± 0.009	0.191 ± 0.031	0.287 ± 0.053
August	0.104 ± 0.013	0.107 ± 0.008	0.360 ± 0.063	0.199 ± 0.025
October	0.073 ± 0.006	0.084 ± 0.005	0.291 ± 0.063	0.336 ± 0.024
December	0.041 ± 0.001	0.082 ± 0.010	0.176 ± 0.026	0.338 ± 0.020

In addition, metastable iron oxide phases such as goethite may take long periods of time to convert to hematite. Finally little thermodynamic data for iron oxides other than magnetite and hematite exists, and is therefore not incorporated into databases such as the one used in the study of Cornell and Schwertmann (2003).

The amount of Fe_{HR} at CBC remains constant in March and April, decreasing in May, as do the Fe_T and Fe_R levels. The decreased levels of reactive iron oxides may reflect the slowing of bottom currents due to reduced discharge in the summer and autumn, resulting in less sediment resuspension, or may reflect consumption by heterotrophic bacteria in the sediment layer. The opposite trend occurs at GP,

Table 6: Pyrite extraction results (wt% Fe).

Month	CBC	*GP*
March	0.4%	0.6%
April	–	0.5%
May	0.4%	0.5%
June	0.4%	-
August	0.3%	0.6%
October	0.4%	0.7%
December	0.3%	0.2%

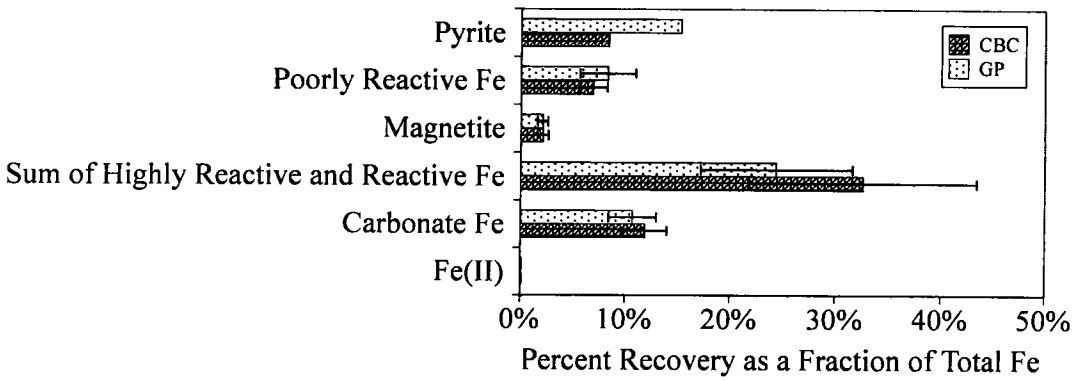

Figure 8: CBC and GP Extraction results, as a percent of Fe_T. The highly reactive and reactive fractions were combined.

as Fe_{HR} increases between March and April, decreases during early summer, and increases in August. Fe_T mimics highly reactive and reactive iron concentrations, but the same is not observed when examining the other iron minerals. It is possible that trends are only apparent when examining Fe pools that make up a relatively large fraction of Fe_T, as these trends are less likely to be masked by lower mineral concentrations and variable recoveries.

When concentrations of Fe_{HR} and Fe_R are combined and examined as a percentage of Fe_T, total reactive iron at CBC was 28-35% of the total iron, and reactive iron

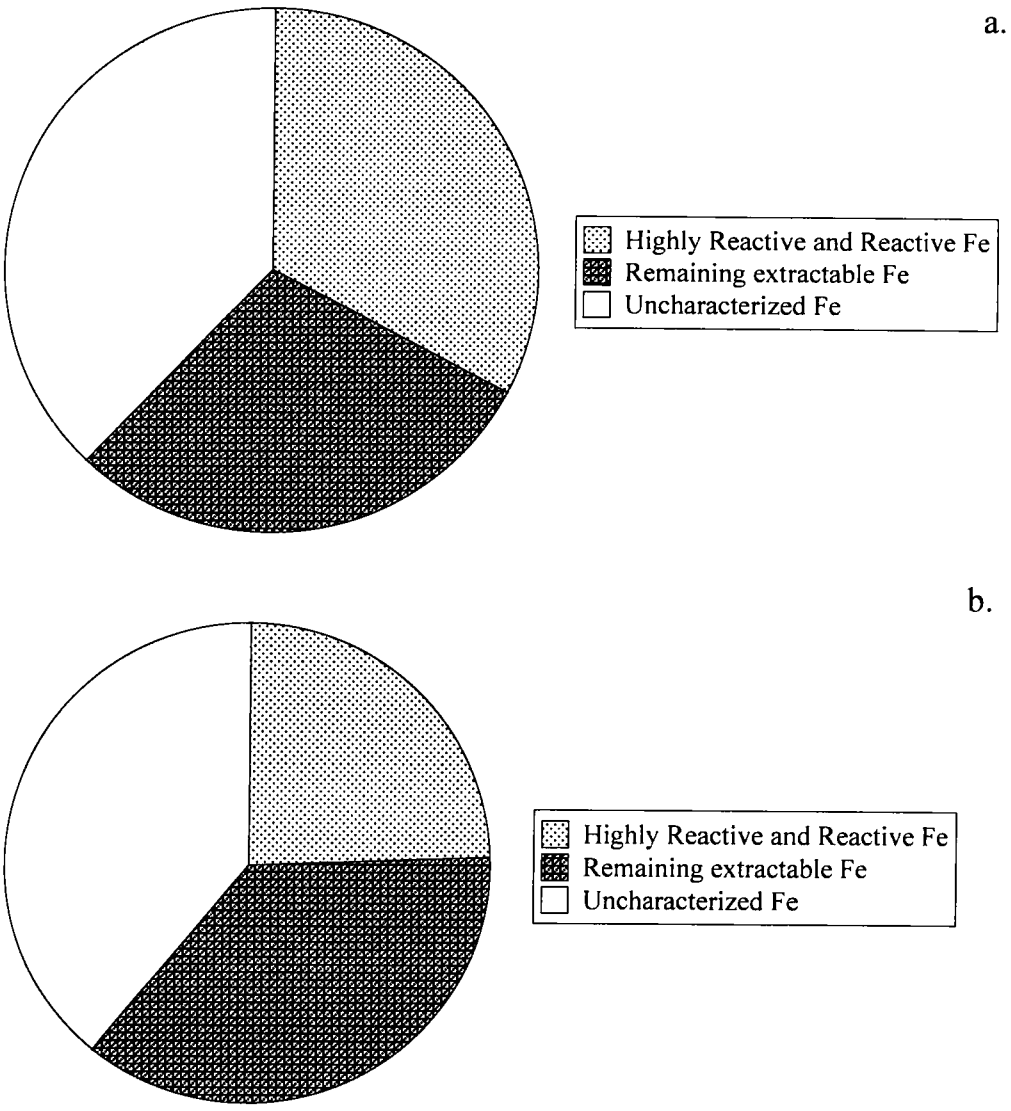

Figure 9: Average of reactive Fe, undefined Fe and remaining reactive Fe at (a) CBC and (b) GP.

concentrations at GP were 20-30% of the total Fe (Fig. 8). These two fractions of reactive iron comprise one half of the iron extracted using the extraction sequence and the pyrite extraction technique (Fig. 9).

The cumulative sum of iron concentrations resulting from the five-stage extraction process, plus the Fe(II), and pyrite/AVS extractions were less than the concentration of total iron obtained through ashing for each site over the sample period; on average,

Table 7: Undefined Iron, representing the difference between the total Fe determined though ashing and the amount of Fe extracted through the five-step process, Fe(II) and pyrite extractions (when available).

	Fe_U (wt% Fe)		Fe_U as % of Fe_T	
Month	GP	CBC	GP	CBC
March	1.6 ± 0.10	1.3 ± 0.30	45.6 ± 0.07	31.6 ± 0.25
April	1.3 ± 0.20	2.5 ± 0.12	38.2 ± 0.17	56.8 ± 0.05
May	1.4 ± 1.02	1.3 ± 0.51	42.4 ± 0.79	35.1 ± 0.42
June	1.2 ± 0.21	1.4 ± 0.31	49.9 ± 0.19	35.8 ± 0.23
August	0.9 ± 0.90	1.6 ± 0.33	25.6 ± 1.04	40.0 ± 0.22
October	1.3 ± 1.20	2.4 ± 0.50	37.1 ± 0.99	53.3 ± 0.24
December	0.66 ± 0.31	2.0 ± 0.21	34.6 ± 0.49	44.3 ± 0.11

Table 8: Extraction efficiencies and undefined Fe, December CBC. Possible Fe concentrations were calculated by dividing the extracted Fe concentration by the lowest extraction efficiency (taken from Table 3), determining the maximum amount of Fe which could have been extracted. For Fe_{HR}, which is thought to contain ferrihydrite and lepidocrocite, the value used to calculate the maximum possible concentration is the lower of the two extraction efficiencies in Table 3. The same process was used to calculate the maximum concentration of Fe_R, which is thought to contain goethite and hematite. Extraction efficiencies were not calculated for Fe_C, Fe_{PR}, and pyrite. All concentrations are wt% Fe. Fe_T in December at CBC is 4.5 $\pm$ 0.2 wt%

Fe fraction	Extracted Fe Concentration	Maximum Possible Concentration
Fe_{HR}	0.7	0.92
Fe_R	0.6	1.15
Fe_M	0.04	0.04
Fe_{PR}	0.2	
Fe_C	0.3	
Pyrite	0.3	
Total:	2.14	2.91
Fe_U (Fe_T-$Fe_{maximum}$)		1.59
Fe_U (Fe_T - $Fe_{Extractions}$)		2.36

3.2 X-RAY DIFFRACTION ANALYSIS

X-ray diffraction analysis was performed in an effort to characterize undefined sedimentary iron through identification of mineral phases present in the samples. X-ray diffraction results analyzed using Rock Jock software (Eberl, 2003) resulted in a quantitative and qualitative analysis of clays and other minerals in the samples. Chert and quartz were the main components of the sediment sample, and ferrihydrite, lepidocrocite, and pyrite were also observed (Tables 9 and 10). Conversely, hematite, magnetite, and goethite were not detected in samples using XRD analysis, in contrast with the results obtained by the chemical extraction. The XRD peaks obtained from the predominant minerals in these samples (e.g. quartz and chert) may be responsible for masking iron minerals that are present at lower concentrations in the sample. It is also possible iron minerals are nano-sized particles which do not produce discernible peaks (van der Zee et al., 2005). In addition, uncertainty exists in the calculation program, as the clays and minerals standards used for analytical comparison may have different structures or impurities than the clays and minerals in the York River sediments.

The XRD clay analysis of the March CBC sample attributed 1.5 wt% Fe to clay phases and amphibole (ferroschermakite), a figure very close to the amount of uncharacterized Fe (1.43%) (Table 9) determined during chemical extractions. Based on XRD total amount of Fe present in the sample, the sum of reactive Fe minerals and Fe in clays was 5.5 wt% Fe, a value within 25% of the amount of Fe determined through ashing. In addition, XRD analysis and chemical extraction values were also similar for pyrite. The analysis did not agree with the Fe_{HR}, Fe_R, and Fe_M chemical extraction results.

The March CBC sample was also analyzed without the corundum standard added (Table 9), as were samples taken from CBC in August and GP in June (Table 10). Most samples had been analyzed prior to obtaining the USGS software and XRD analysis began at 10°; RockJock requires XRD input reflections to begin at 5° and end at 65°, and the March CBC sample with the corundum standard was analyzed beginning at 5°. The analysis examines the reflection values beginning at 19°, but the program can be instructed to examine the data between 5° and 19° to differentiate between similar patterns (Eberl, 2003). The addition of the standard produces results which vary from the standardless patterns. The two March CBC sample analytical results were quite different, with the exception of Fe-rich chlorite,

pyrite, and glauconite, whose concentrations of Fe were the same or almost identical (Table 9). The total iron determined using XRD with a corundum standard was 20% higher than the total iron determined by ashing, and 39% lower in the sample analyzed without a corundum standard. The August and June samples analyzed without the corundum standard were 48% and 10% lower than the total Fe determined by ashing (Table 10).

Fe_U and its potential relationship to the clay fraction was examined by calculating a hybrid Fe_T concentration by combining the sum of the Fe derived from the chemical extractions with the sum of the XRD derived clay concentrations (Tables 11 and 10). For the March CBC, June GP, and August CBC samples, the Fe_T concentration determined through the hybrid calculation was much closer than the total Fe concentration derived from ashing (Tables 9 and 10), further supporting the conclusion that clays make up much of the undefined portion of Fe in the CBC and GP samples (Fig. 9).

The sediment particles examined originate in different areas of the watershed and were subjected to a variety of physical and chemical weathering processes prior to deposition in the York River. It is possible that the accuracy of XRD results could be increased by collecting and analyzing minerals collected at possible source regions within the watershed, and importing their reflection data into the Rock Jock program.

3.3 MÖSSBAUER SPECTROSCOPY

To further assess the validity of the XRD analysis, results of Mössbauer spectroscopy (MS) at 300 K and 77 K were were compared to those obtained from the Rock Jock XRD calculations (Table 11, Figs. 10, 11, 12). Clay and mineral concentrations based on XRD analysis were used to determine the amount of Fe(II) and Fe(III) present in the March CBC sample. This information was used in conjunction with the chemical composition of each clay or mineral to determine the weight percentages of Fe(II) and Fe(III) in the sediments.

The amount of Fe(II) and Fe(III) estimated from MS analysis was compared to that obtained through XRD analysis for March and August CBC samples. Due to the amount of sediment required for XRD, it was not possible to compare all samples analyzed using MS. March CBC and August CBC samples were analyzed in both instruments, and the amount of Fe(II) and Fe(III) was similar for both methods (Table 12). The composition of Fe(II) and Fe(III) in the clays and minerals found by

XRD when analyzing the March CBC sample are 27% Fe(II) and 73% Fe(III). When examining the August CBC sample, the concentration of Fe(III)estimated using MS is less than 10% (absolute) higher than the concentration estimated using XRD analysis.

Table 9: XRD and Chemical Extractions: March CBC with and without corundum standard addition (wt % Fe).

Mineral (All values expressed as wt%)	XRD: with Corundum Standard[a]	XRD: without standard[a]	Chemical extraction	Hybrid Analysis (with Standard)	Hybrid Analysis (without Standard)
Fe_{HR}	4.13	0.35	0.77	0.77	0.77
Fe_R	0.00	0.00	0.66	0.66	0.66
Fe_M	0.00	0.00	0.08	0.08	0.08
Fe_C			0.59	0.59	0.59
Pyrite	0.19	0.14	0.36	0.36	0.36
Total (iron oxides plus pyrite)	4.32	0.50	2.46	2.46	2.46
Fe_U (Fe_T - $Fe_{Extractions}$)			1.64	1.64	1.64
XRD Clay analysis					
Fe_{PR}			0.21		
Smectite (Saponite)	0.23	0.10		0.23	0.10
Smectite (Ferruginous)	0.67	1.30		0.67	1.30
Illite	0.09	0.11		0.09	0.11
Biotite	0.00	0.13		0.00	0.13
Chlorite (Cca-2)	0.01	0.00		0.01	0.00
Chlorite (Fe-Rich)	0.00	0.00		0.00	0.00
Ferrotschermakite	0.24	0.96		0.24	0.96
Glauconite	0.26	0.00		0.26	0.00
Total Clays	1.50	2.62		1.50	2.62
Fe_T	5.82	3.12	4.10	3.14	4.26
Degree of Fit (RockJock)	0.033	0.081			
	Sum of Total Clays, Iron Oxides, and Pyrite	Sum of Total Clays, Iron Oxides, and Pyrite	(Ashing)	Sum of chemical extraction and XRD analysis[b]	Sum of chemical extraction and XRD analysis[b]

[a]XRD values for functional groups are determined by adding the mineral fractions determined through RockJock analysis.

[b]The hybrid analysis combines the chemical extraction results with the XRD clay results. For the purpose of this comparision, Fe_{PR} was considered to be part of the clay fraction and was not included in the extractable Fe sum.

Table 10: XRD and Chemical Extractions: August CBC and June GP, without corundum standard addition (wt % Fe).

Mineral (All values expressed as wt%)	XRD: August CBC[a]	Chemical extraction: August CBC	Hybrid Analysis, August CBC	XRD: June GP[a]	Chemical Extraction: June GP	Hybrid Analysis, June GP
Fe_{HR}	0.35	0.71	0.71	0.77	0.45	0.45
Fe_R	0.00	0.67	0.67	0.00	0.30	0.30
Fe_M	0.00	0.11	0.11	0.00	0.05	0.05
Fe_C		0.43	0.43		0.25	0.25
Pyrite	0.19	0.25	0.25	0.37		
Total (iron oxides plus pyrite)	0.54	2.17	2.17	0.77	1.05	1.05
Fe_U (Fe_T - $Fe_{Extractions}$)		1.59			1.19	
XRD Clay analysis						
Fe_{PR}		0.19			0.19	
Smectite (Saponite)	0.00		0.00	0.00		0.00
Smectite (Ferruginous)	0.32		0.32	0.41		0.41
Illite	0.06		0.06	0.11		0.11
Biotite	0.00		0.00	0.00		0.00
Chlorite (Cca-2)	0.01		0.01	0.01		0.01
Chlorite (Fe-Rich)	0.00		0.00	0.00		0.00
Ferrotschermakite	0.00		0.00	0.00		0.00
Glauconite	0.20		0.20	0.25		0.25
Total Clays	0.59		0.59	0.78		0.78
Fe_T	1.13	3.96	2.76	1.55	2.43	1.83
Degree of Fit (RockJock)	0.08			0.05		
	Sum of Total Clays, Iron Oxides, and Pyrite	(Ashing)	Sum of chemical extraction and XRD analysis[b]	Sum of Total Clays, Iron Oxides, and Pyrite	(Ashing)	Sum of chemical extraction and XRD analysis[b]

[a] XRD values for the functional groups are determined by adding the mineral fractions determined through RockJock analysis

[b] The hybrid analysis combines the chemical extraction results with the XRD clay results. For the purpose of this comparision, Fe{PR} was considered to be part of the clay fraction and was not included in the extractable Fe sum.

Table 11: MS Comparison of Fe(II) and Fe(III).

	CBC March (77 K)	CBC March A (300 K)	GP Dec (77 K)	GP Dec (300 K)	GP March (300 K)	CBC August (300 K)
Fe(II)	15.77	15.32	19.02	19.02	19.98	16.04
Fe(III)	84.23	84.68	81.3	80.98	80.02	83.96

Table 12: Comparison of Fe(II) and Fe(III), as derived through XRD and MS.

CBC March	CBC March (77 K)	CBC March (300 K)	XRD March CBC (with standard)	Hybrid XRD and Extraction (with standard)
Fe(II)	15.77	15.32	8.80	32.79
Fe(III)	84.23	84.68	91.20	67.21

CBC March	CBC March (77 K)	CBC March (300 K)	XRD March CBC (without standard)	Hybrid XRD and Extraction (without standard)
Fe(II)	15.77	15.32	16.50	28.74
Fe(III)	84.23	84.68	83.50	71.27

CBC August	CBC August (300 K)	XRD August	Hybrid XRD and Extraction
Fe(II)	16.04	24.9	31.80
Fe(III)	83.96	75.1	66.20

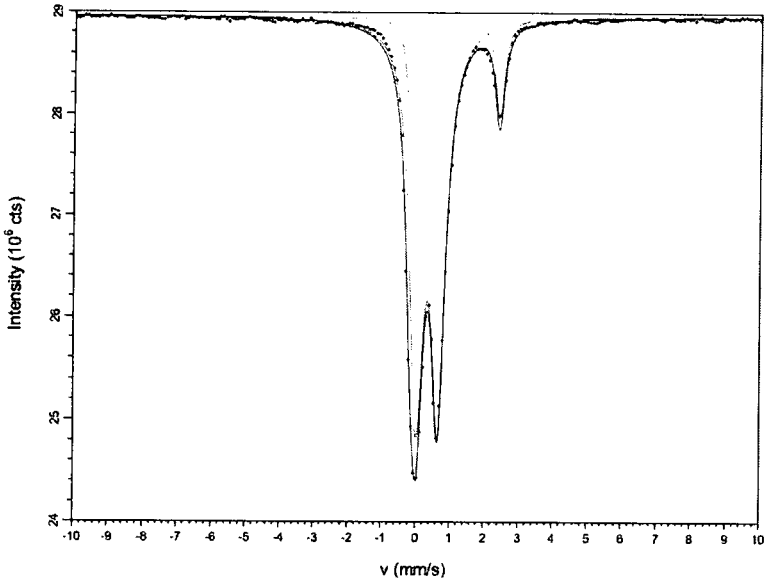

(a) 300 K Mössbauer, March CBC

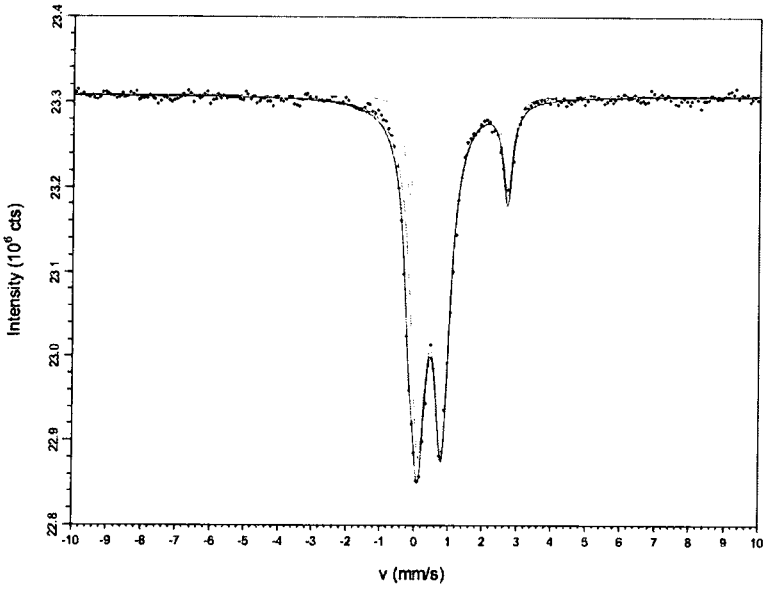

(b) 77 K Mössbauer, March CBC

Figure 10: Mössbauer results, March CBC. The smaller of the two doublets in each image represents Fe(II), and the longer doublet represents Fe(III).

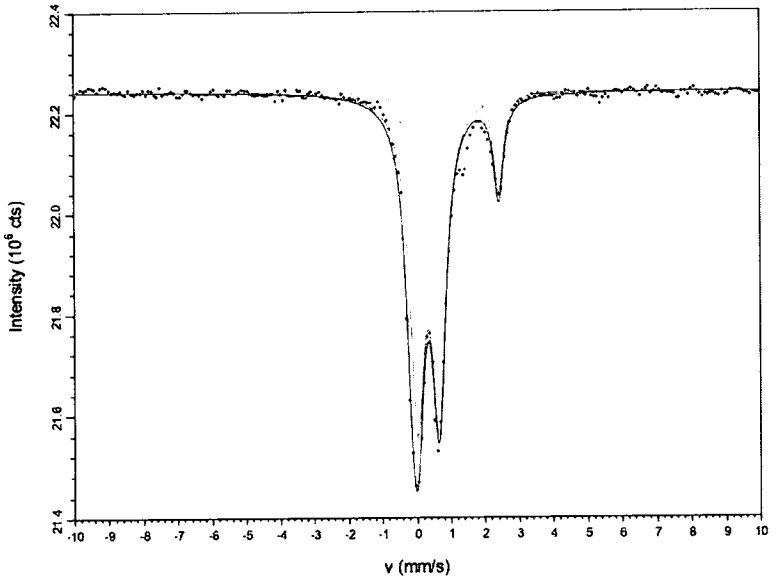

(a) 300K Mössbauer, December GP

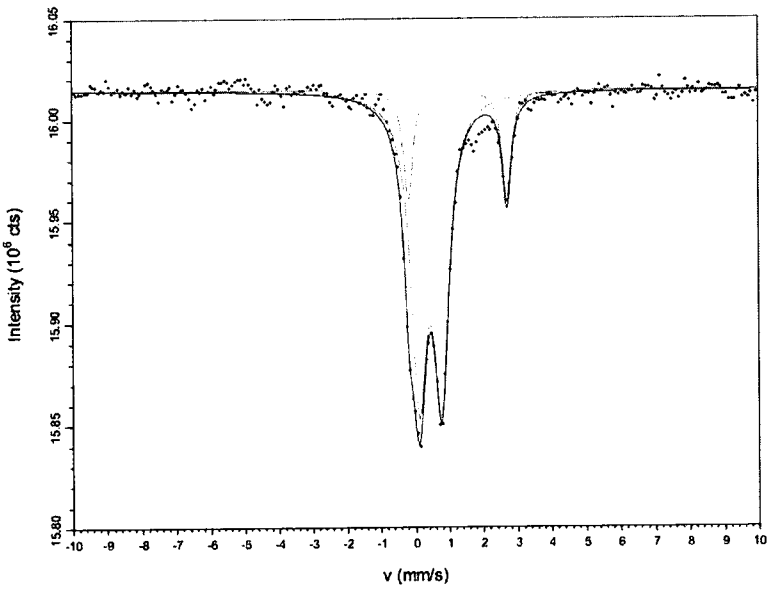

(b) 77 K Mössbauer, December GP

Figure 11: Mössbauer results, December GP. The smaller of the two doublets in each image represents Fe(II), and the longer doublet represents Fe(III).

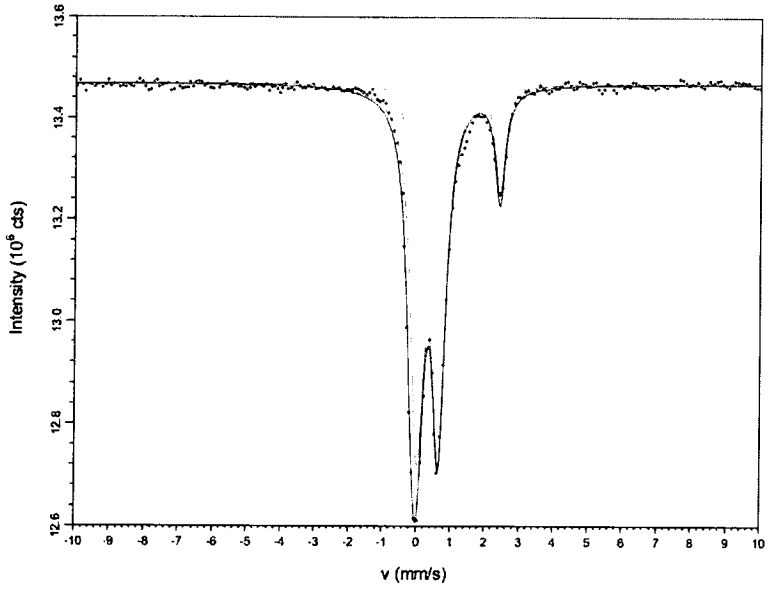

(a) 300 K Mössbauer, March GP

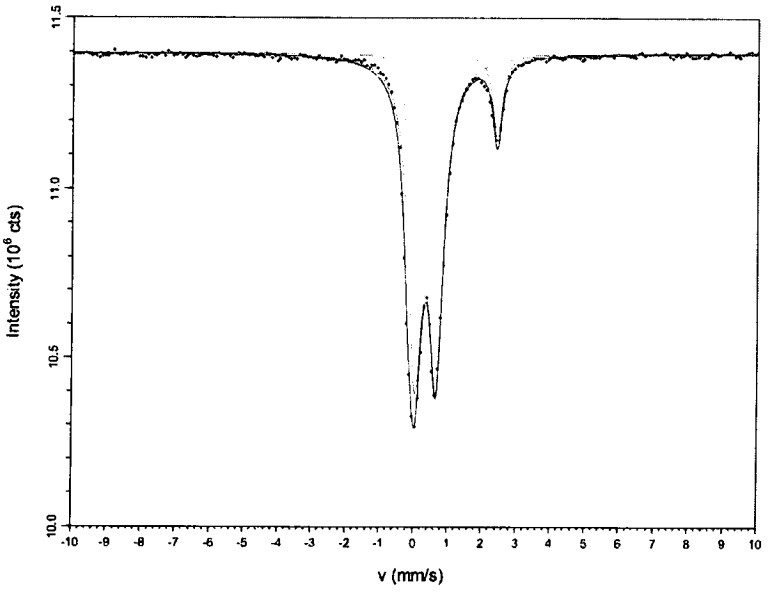

(b) 77 K Mössbauer, August CBC

Figure 12: Mössbauer results, March GP and August CBC. The smaller of the two doublets in each image represents Fe(II), and the longer doublet represents Fe(III).

CHAPTER 4

DISCUSSION

4.1 IRON OXIDES AT CLAY BANKS CHANNEL AND GLOUCESTER POINT

York River water column physical and biological processes appear to impact the amount of reactive iron observed in the sediments. Ferrihydrite and lepidocrocite concentrations are highest during the spring bloom at both GP and CBC. Further, the concentration of highly reactive iron is always higher at CBC (Fig. 5), and burial of organic matter is not observed at CBC during the study period (Palomo and Canuel, 2010). However, the differences between iron concentrations at each site varies throughout the year (Fig. 4) and more observations over a longer period may reveal more definitive patterns.

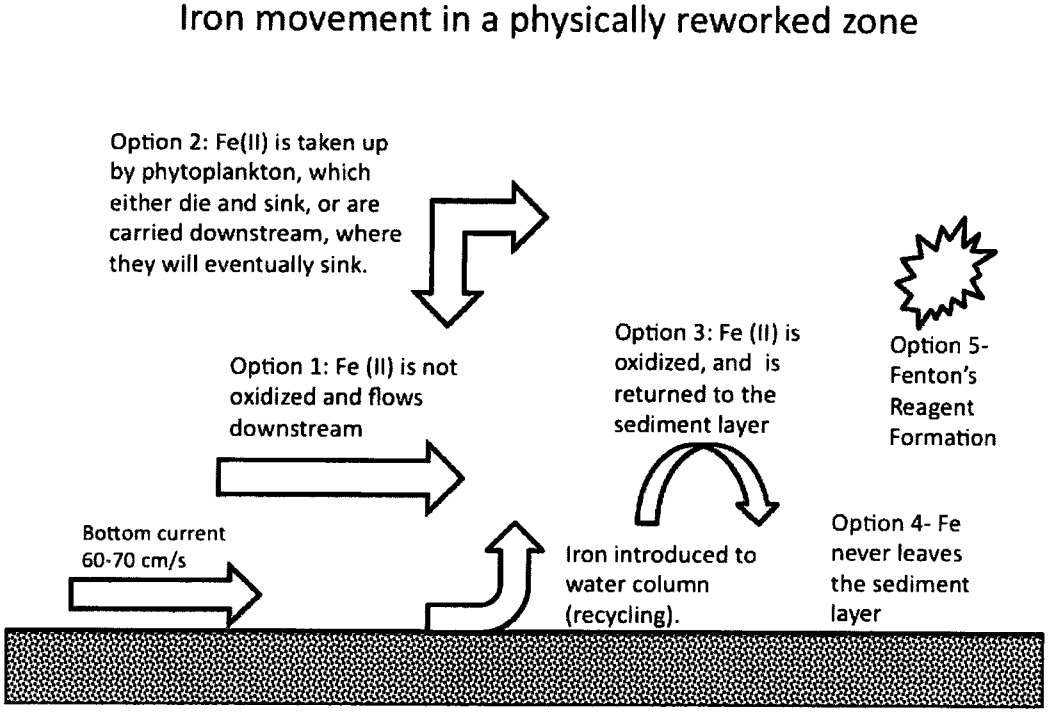

Figure 13: Potential pathways for Fe at physically reworked site. The illustration examines theoretical iron movement within the CBC channel.

Greater physical reworking at the CBC site allows a greater potential for the "recycling" of iron particles in that older iron particles, such as hematite and magnetite, or iron absorbed to clay surfaces, may be converted into highly reactive iron oxides such as lepidocrocite and ferrihydrite (Raiswell, 2011). This process is much less important at GP, where bioturbation introduces oxygen to the sediments, but only where a burrowing organism disturbs the sediment surface. The oxygen introduced into the sediment layer is somewhat localized at GP, and any iron oxides formed as a result of the presence of O_2 are unlikely to enter the water column or move past the site of O_2 introduction. At CBC, an iron particle may enter the water column, travel downstream, stay in its original location, or be used to form Fenton's Reagent and degrade refractory organic matter (Fig. 13). It is difficult to determine the relative importance of each scenario as this study only examined surface sediments collected at the site and did not analyze water column samples. The first two options in figure 13 will most likely result in an increase of OM in the river or in the estuary, depending on the distance the Fe(II) or the organism which takes up Fe(II) travel. In scenario 3, Fe(III) may be utilized as an electron acceptor, and if the Fe(III) is utilized by heterotrophic bacteria, OM degradation may result. Scenario 4 may result in the same outcome as scenario 3, depending on the type of Fe present and the ability to oxidize Fe(II). Finally, in scenario 5, the formation of Fenton's reagent does not impact the iron recycling process, as the iron(II) oxidized during the first part of the reaction is then reduced when remineralizing organic matter (Burdige, 2006; Hedges and Keil, 1995), but can change the concentration of OM through the remineralization of refractory organic matter.

The transient nature of CBC sediments has been documented and particle residence times in the channel are negligible (Dellapenna et al., 1998). Residence times of sediments in the river average 200 years (Dellapenna et al., 1998), which suggests reactive iron formed at the site may move to other areas of the river. The presence of heterotrophic bacteria offers the possibility that Fe is utilized as an electron acceptor in the degradation of OM. Finally, Fenton's Reagent forms spontaneously and data is not available to determine the extent that Fenton's Reagent may degrade OM in the study area. The presence and quantity of H_2O_2 at GP and CBC has not been measured.

Observed seasonal variation in Fe_{HR} and Fe_R may be attributed to suspended biomass in the water column utilizing Fe(II) for microbial processes during blooms,

and in the case of CBC, the bottom current velocity. The increased concentration of polyunsaturated fatty acids (PUFAs) at CBC during the spring and the absence of preserved OM may indicate Fe plays a significant role in remineralizing carbon at the location. Fe(III) is present at GP in smaller quantities (Table 11), but since the surfaces sediments are not resuspended in the manner of CBC sediments, oxygen may consistently penetrate the sediment surface to allow Fe(II) to reoxidize to highly reactive Fe(III).

Evidence that Fe(III) may play a role in OM remineralization at CBC stems from the increased amount of heterotrophic bacteria at CBC. These data agree with the findings of Aller (1998) where he demonstrated that areas experiencing great physical reworking also had the smallest concentrations of buried organic matter. All of the areas sampled within the mobile mud belt in the Amazon River basin had significantly greater bacterial biomass than two bioturbated sites included in the study, locations where macrofauna dominates. The Aller (1998) study also indicated that redox cycling of Fe and Mn dominates the physically reworked sediments, and that OM from marine sources is consumed at greater rates than terrestrial OM. It is unlikely Fe is the only electron acceptor present in the York River sediments, but it is possible Fe was significantly utilized to remineralize OM as an electron acceptor.

Grain size is often assumed to be the predominant controlling factor of the amount of Fe in sediments (Poulton, 2003; Horowitz and Elrick, 1987). Each site in this study consists of silty muds, but the SSA at CBC was larger than that at GP (Table 1. While Fe_T was not different at either site when concentrations were normalized to SSA, Fe_{HR} and Fe_R were both higher at CBC. As expected, weak currents at GP, near the mouth of the river, result in an average SSA lower than that of CBC, indicating larger grains being deposited at the CBC site. The larger grains would presumably have lower sediment surface area, and as a result sediments would have lower Fe concentrations; during the study period this is most apparent during the month of June (Tables 1 and 4) . Since extremely rapid bottom currents do exist at CBC, smaller sediments are deposited, which results in greater surface area for Fe adsorbtion to the sediment surface. The resuspension of these sediments allows for Fe cycling and the potential for OM remineralization.

Iron concentrations at both CBC and GP agree well with those observed at other sites experiencing strong physical reworking or bioturbation (Table 14). The effect of temperature seems less pronounced than that of site dynamics such as bottom current

Table 13: Comparison of Chesapeake Bay Tributary Sediment Surface Area to wt%.

Location	Fe (wt%)	SSA m^2g^{-1}	Fe ($mg{\cdot}m^{-2}$)
Patuxent River at Hog Point (Horowitz and Elrick, 1987)	3.0	9.9	3.0
Patuxent River at Point Patience (Horowitz and Elrick, 1987)	2.3	7.9	2.9
Patuxent River at St. Leonard's Creek (Horowitz and Elrick, 1987)	4.2	15.1	2.8
Clay Bank Channel	4.4	22.7	1.9
Gloucester Point	3.1	18.0	1.7

speed, as only slight differences are seen between Fe concentrations in sediments found in tropical versus temperate settings (Aller et al., 2004; Aller, 2004).

When comparing the results from the two York River sites to those from previous studies, the areas experiencing the greatest bottom currents have the highest concentrations of reactive iron, as seen in at CBC. It should be noted that different studies define the mineral species that compose reactive iron differently, and one definition may include ferrihydrite, lepidocrocite, goethite and hematite, while another study may only include ferrihydrite and lepidocrocite in the definition of reactive iron. In addition, not all studies measure reactive iron over a temporal scale, when river discharge is responsible for the physically reworked study area. As a result, average concentrations in such studies may be lower than those in other studies because seasonal differences in river discharge may affect levels of reactive iron in physically disturbed sediments. To examine the potential for increased concentrations of Fe in CBC sediments, SSA and Fe_T measurements from the Patuxent River (Horowitz and Elrick, 1987), a northern tributary of the Chesapeake Bay, were compared to York River measurements (Table 13). The Patuxent River sites suggest that similar amounts of Fe coat grains of larger size than those found at CBC or GP, meaning that more Fe could coat York River grains if enough iron were present in the system. One may assume from these comparisons that sediment size is not a factor limiting iron concentrations, and physical reworking versus bioturbation is responsible for the greater amount of Fe found in the sediments.

The magnitude of physical reworking does appear to have an impact on total iron concentrations in sediments, as the areas with the greatest reworking have the highest concentrations of total iron and reactive iron oxides (Table 14). Currents at the Clay Bank site are slower than bottom currents observed at the Amazon Delta and Gulf of Papua, two of the most extremely reworked settings described in literature, but the iron concentrations in the CBC sediments are only slightly lower than those measured in the tropical sites. Weathering regimes, source material, and the distance the source material travels (which will affect the amount of weathering) prior to entering the physically reworked system may help to further explain the differences in Fe concentrations.

Table 14: Comparison of Sediment Iron Concentrations Measured in Tropical and Temperate Climates.

Site	Total Fe (mg Fe/g sed)	Reactive Fe (mg Fe/g sed)	Type of Mixing
Central Long Island Sound (Aller, 1994)		0.92%	Biological
FOAM Site (Canfield, 1989)	2.20%	0.56%	Biological
Cape Hatteras (Aller, 2004)	3.40%	0.95%	Biological
Eel Delta (N. California) (Sommerfield et al., 2001)		0.84%	Physical
Amapa, Brazil Coast (Aller, 2004)		2.12%	Physical
Mississippi Delta (Aller, 2004)	4.30%	0.85%	Physical
Gulf of Paupa (Aller, 2004)	4.47%	2.02%	Physical
Amazon Delta (Aller and Blair, 1996)	5.31%	1.62%	Physical
French Guiana (Aller, 2004)	4.70%	2.09%	Physical
Gloucester Point (Average)	3.11%	0.75%	Biological
Gloucester Point (Maximum)	3.5%	1.04%	Biological
Clay Bank (Average)	4.40%	1.35%	Physical
Clay Bank (Maximum)	4.5%	1.46%	Physical

4.2 ANALYTICAL TECHNIQUES

X-ray diffraction and MS are powerful tools to use when determining the distribution and speciation of Fe in marine sediments, and the agreement with the chemical extractions suggests that non-destructive analytical methods may be useful for determining iron concentrations in certain settings (Tables 9, 10, and 12). X-ray diffraction proved to be a valuable tool when used to examine the uncharacterized iron in the sediments, but XRD analysis alone is not adequate for characterizing the complex muds found in the York River. The analysis can result in 'false positives' for certain minerals and clays (Eberl, 2003), and minerals or clays with signatures similar to the dominant minerals in the sediment may be masked by those mineral patterns.

Using the corundum standard does appear to increase the accuracy of the XRD RockJock analysis. Accuracy is measured by degree of fit, using a whole-pattern fitting program which compares integrated intensities to standards to determine best fit. Ideal degree of fit values are less than 0.100, and the parameter describes the agreement between the sample and the standards examined (Eberl, 2003). When analyzing the March CBC sample containing the corundum standard, the degree of fit was always <0.100 (0.033) when a constant background correction was applied by the program (Table 9). The March CBC sample and August CBC samples analyzed without the corundum standard both had degree of fit parameters were both 0.08; the June GP sample was 0.05 (Table 10). Agreement between the March sample containing the corundum standard and the June sample with the chemical extraction data was much closer than the agreement between the March CBC (without a corundum standard) and August CBC XRD and extraction results. Inconsistencies between XRD and extraction data may result from the difficulties detecting amorphous phases of iron in samples by XRD (van der Zee et al., 2005). In addition, XRD is best utilized when sediment source rocks in the watershed are identified and when local samples of watershed rocks and clays can be used to create standards to match to the sample (Eberl, 2003). This study did not analyze local samples for the project, instead utilizing the Rock Jock standards.

The results described in Table 12 were further examined in an attempt to determine the difference between the percent of Fe(II) and Fe(III) determined through the hybrid and MS analyses. Fe_T concentrations obtained through ashing was considered

first, as an error in the total Fe could skew the ratio of Fe(II) to Fe(III). Examination of Fe_T determinations in other coastal settings including other sites within the Chesapeake Bay (Aller et al., 2004; Horowitz and Elrick, 1987) showed agreement with the CBC and GP values, and it was determined that large errors were unlikely in the Fe_T analysis by ashing. The possibility of Fe minerals other than iron carbonates being extracted during the sodium acetate extraction was not considered based on attempts to extract synthetic ferrihydrite and magnetite using a pH 4.5 sodium acetate solution (Table 4). In each case, very little Fe was extracted, as predicted in Poulton and Canfield 2005.

Error in the ratio of Fe(II) to Fe(III) determined through XRD analysis was examined by comparing the ratio of Fe(II) to Fe(III) determined through analysis of Chesapeake Bay clays by Goldberg et al. (1978) and through RockJock clay analysis of the sediments. These ratios were applied to the uncharacterized Fe in Tables 9 and 10, and agreement between MS analysis and these ratios was not achieved. The next consideration to be made was the possibility the Fe(II) in the clays was oxidized during the freeze drying process and during storage plus analysis, as has been observed in other studies of iron distributions in marine sediments (Drodt et al., 1997; Kïg et al., 1997; König et al., 1999). The assumption was therefore made that all Fe(II) in the clays here had oxidized, and any Fe(II) in the sediment samples was derived solely from Fe_C and pyrite (Table 15). Comparing the Fe(III) which would result from oxidized clay minerals and that obtained from extraction results to those determined through MS analysis resulted in very close agreement (Table 15). The oxidation of Fe in clays may explain not only the difference between the Fe(II) and Fe(III) in the hybrid calculation and the MS analysis, but also the difference between MS analysis and the ratio of Fe(II) to Fe(III) predicted by combining the chemical extraction data and the expected ratio of Fe(II) to Fe(III) in Chesapeake Bay clays (Goldberg et al., 1978).

Magnetite and the other iron minerals were not detected at 300 K and 77 K Mössbauer Spectroscopy, but Fe(II) and Fe(III) were detected (Figs. 10, 11, and 12). The iron present is most likely composed of nano-particles too small to become paramagnetic at these temperatures, or consists of poorly crystalline structures that do not become paramagnetic until 4 K. If nano-particles are present, the 300 K and 77 K data is still valid; the 300 K and 77 K data provides the proportion of Fe(II) and Fe(III) in the sample. It is likely analysis at 4 K would reveal the speciation

Table 15: Fe(II):Fe(III) Analysis of CBC and GP Sediments.

	MBR (wt %)[a]	Hybrid (wt %)[a]	Clay Ratio 4:1[b] (wt %)	Clay Ratio 1:1 (wt %)	Clay Ratio 0:1 (wt %)
March CBC					
Fe(II)	15.3	32.8	46.2	43.8	23.8
Fe(III)	84.7	67.2	53.8	56.2	76.2
Total Fe	–	3.1	4.1	4..1	4.1
August CBC					
Fe(II)	16.0	31.8	48.1	40.6	18.0
Fe(III)	84.0	66.2	51.9	59.4	82.0
Total Fe	–	2.8	4.0	4.0	4.0
December GP					
Fe(II)	19.0	–	39.2	49.3	26.4
Fe(III)	81.0	–	60.8	50.7	73.6
Total Fe	–	–	1.9	1.9	1.9
March GP					
Fe(II)	20.0	–	32.0	45.8	26.8
Fe(III)	80.0	–	68.0	54.2	73.2
Total Fe	–	–	3.5	3.5	3.5

[a]Data from Tables 11 and 12.

[b]Ratios are Fe(II):Fe(III). 4:1 Ratio from Goldberg et al., 1978, 1:1 ratio from RockJock analysis of the XRD data in Tables 9 and 10.

of the iron in the sample, resulting in more accurate information regarding the concentrations of the minerals. If the nano-particles were resolved at 4 K, Mössbauer Spectroscopy would become a preferred method of analysis as it can also determine concentrations of minerals present. As a result, combining MS with traditional chemical extractions could provide a greater understanding of nano particles and larger Fe minerals in physically and biologically reworked areas. The recently documented presence of nanogoethite in Mediterranean and lacustrine sediments was unexpected, and suggests that microbial processes in an oxic sediment-water interface are not completely understood, in that ferrihydrite may not be the primary electron acceptor utilized by bacteria in marine environments (van der Zee et al., 2005, 2003).

CHAPTER 5

CONCLUSIONS

The first question posed in this study addressed the concentrations of reactive iron oxides in physically reworked and bioturbated sites. Chemical extraction results showed relatively constant amounts of reactive iron oxides over a ten month period at both CBC and GP, both when Fe concentrations are expressed as a weight percentage of the sediments or when normalized to surface sediment area. Fe_{HR} and Fe_R were always higher at the physically reworked CBC site, even during periods of decreased river discharge which resulted in weaker bottom currents. The presence of amorphous Fe phases such as ferrihydrite suggests the rapid cycling of iron. If the cycling of iron took place on a longer time scale, it is more likely the oxides would transform into more crystalline species of Fe (Schwertmann and Murad, 1990). The increased concentrations of Fe_{HR} and Fe_R at CBC are potentially due to the swift bottom currents. Bioturbation is thought to be the predominant means of introducing O_2 into GP sediments versus physical reworking, and the reduced exposure to O_2 at GP (compared to CBC) may explain the lower concentrations of reactive Fe at GP compared to CBC. Overall, the results of this study agree with studies of reactive iron oxides found in physically reworked and bioturbated areas in both temperate and tropical climates, and the iron cycling that results from reworking and bioturbation could potentially play an important role in organic matter remineralization in other physically reworked areas in estuaries along the continental shelf.

The study also examined the role of reactive iron on the increased organic remineralization observed by Palomo and Canuel (2010). Reactive iron at CBC may be a result of heterotrophic bacteria remineralizing organic matter, using Fe as an electron acceptor. The reduced iron may become reoxidized during physical reworking, but additional data needed to link the processes is required. Arzayus and Canuel (2005) examined refractory OM at GP and CBC and found the concentration of refractory OM at CBC was greater than at GP. The authors suggest this could be a result of greater exposure to O_2 and to electron acceptors in the water column (i.e. Fe or Mn); however, the presence of electron acceptors other than Fe has not been studied.

The third question posed in this study regards flow variation and biological processes on the concentrations of reactive iron oxides. Clear temporal trends in sedimentary Fe distribution were not easily identified during this study, and examination

of the sites over a longer time frame with more frequent sampling would help clarify system dynamics. Greater concentrations of highly reactive iron oxides were present at CBC during peak discharge periods, and the concentrations were significantly different from concentrations of highly reactive iron at GP over the study period. The concentrations of Fe_{HR} at GP increased in August and October, then decreased in December, possibly a result of storm events which resulted in deep mixing of the sediment layer, rather than bioturbation. As with CBC, concentrations of highly reactive iron oxides at GP did not vary significantly over the study period.

When compared to similar sized grains from other sites within the Chesapeake Bay where greater percentages of reactive Fe were able to form on the sediment surfaces, it appears that grain size was not a controlling factor in reactive iron oxide concentrations at each site (Horowitz and Elrick, 1987). The concentrations of total Fe at CBC were comparable to those measured in Amazon Basin and Gulf of Papua sediments, suggesting differences in climate do not strongly affect total iron concentrations. It is more difficult to compare reactive Fe at the three sites, as the iron extraction procedures varied between studies; a cursory examination of reactive iron concentrations shows similarities between CBC and the tropical sites, and between CBC and the sites in the Mississippi Delta.

The last question to be addressed in this study is the relationship between chemical extraction methods, X-ray diffraction, and Mössbauer spectroscopy. The use of XRD and Mössbauer spectroscopy in this study allowed for the independent examination of Fe speciation and mineralogy. Clay proportions were estimated from XRD analysis, and helped to explain the difference between concentrations of extractable reactive iron and total iron concentrations determined through sediment ashing and digestion. A weakness of XRD when considering these samples is the possibility nano-sized oxides do not produce visible peaks, and the iron oxides are then masked by signatures resulting from larger sized minerals.

Mössbauer spectroscopy can potentially overcome this limitation because only Fe atoms absorb the radiation from the instrument. Iron concentrations in the York River sediments exceed the minimum concentration required for MS and the technique has great promise when applied to marine sediments. Results obtained at 300 K and 77 K were in agreement as to the amount of Fe(II) and Fe(III) in the samples. The proportion of Fe(II) and Fe(III) determined though MS agreed with the amount of Fe(II) and Fe(III) determined by combining the clay XRD analysis results with the

chemical extraction results. While specific iron minerals were not identified at 300 K and 77 K, it is likely iron minerals can be identified at 4 K based on results from other sediment studies (van der Zee et al., 2003, 2005). An opportunity exists to determine if MS is a more efficient method to determine Fe concentrations in sediment samples. Additionally, if analysis determines iron oxide nano-phases are present, further studies can examine whether if these small particles might play a significant role in iron redox reactions and OM remineralization.

References

Aller, R., 2001. Transport and reactions in the bioirrigated zone, in: Boudreau, B., Jørgensen, B. (Eds.), The benthic boundary layer: transport processes and biogeochemistry. Oxford University Press, pp. 269–301.

Aller, R., 2004. Conceptual models of early diagenetic processes: The muddy seafloor as an unsteady, batch reactor. Journal of Marine Research 62, 815–35.

Aller, R., Mackin, J., Cox, R., Jr, 1986. Diagenesis of Fe and S in Amazon inner shelf muds: apparent dominance of Fe reduction and implications for the genesis of ironstones. Continental Shelf Research 6, 263 –89.

Aller, R.C., 1998. Mobile deltaic and continental shelf muds as suboxic, fluidized bed reactors. Marine Chemistry 61, 143–55.

Aller, R.C., Blair, N.E., 1996. Sulfur diagenesis and burial on the Amazon shelf: Major control by physical sedimentation processes. Geo-Marine Letters 16, 3–10.

Aller, R.C., Hannides, A., Heilbrun, C., Panzeca, C., 2004. Coupling of early diagenetic processes and sedimentary dynamics in tropical shelf environments: the Gulf of Papua deltaic complex. Continental Shelf Research 24, 2455–86.

Alongi, D.M., Tirendi, F., Christoffersen, P., 1993. Sedimentary profiles and sediment-water solute exchange of iron and manganese in reef- and river-dominated shelf regions of the Coral Sea. Continental Shelf Research 13, 287–305.

Arzayus, K.M., Canuel, E.A., 2005. Organic matter degradation in sediments of the York River estuary: Effects of biological vs. physical mixing. Geochimica et Cosmochimica Acta 69, 455–64.

Balzer, W., 1982. On the distribution of iron and manganese at the sediment/water interface: thermodynamic versus kinetic control. Geochimica et Cosmochimica Acta 46, 1153 –61.

Berner, R.A., 1970. Sedimentary pyrite formation. American Journal of Science 268, 1–23.

Boyle, E., Edmond, J., Sholkovitz, E., 1977. The mechanism of iron removal in estuaries. Geochimica et Cosmochimica Acta 41, 1313 –24.

Burdige, D.J., 2006. Geochemistry of marine sediments. Princeton University Press.

Canfield, D.E., 1989. Reactive iron in marine sediments. Geochimica et Cosmochimica Acta 53, 619–32.

Canfield, D.E., Raiswell, R., Bottrell, S.H., 1992. The reactivity of sedimentary iron minerals toward sulfide. American Journal of Science 292, 659–83.

Chester, R., Hughes, M., 1967. A chemical technique for the separation of ferro-manganese minerals, carbonate minerals and adsorbed trace elements from pelagic sediments. Chemical Geology 2, 249–62.

Cook, D., 2005. Spectroscopic identification of protective and non-protective corrosion coatings on steel structures in marine environments. Corrosion Science 47, 2550–70.

Cook, D.C., Peterson, C.E., 2005. Corrosion of submerged artifacts and the conservation of the uss monitor. AIP Conference Proceedings 765, 91–6.

Cornell, R., Schwertmann, U., 2003. The iron oxides: Structure, properties, reactions, occurrences, and uses. Vch Verlagsgesellschaft Mbh.

Cutter, G., Oatts, T., 1987. Determination of dissolved sulfide and sedimentary sulfur speciation using gas chromatography-photoionization detection. Analytical Chemistry 59, 717–21.

Dellapenna, T.M., Kuehl, S.A., Pitts, L., 2001. Transient, Longitudinal, Sedimentary Furrows in the York River Subestuary, Chesapeake Bay: Furrow Evolution and Effects on Seabed Mixing and Sediment Transport. Estuaries 24, 215–27.

Dellapenna, T.M., Kuehl, S.A., Schaffner, L.C., 1998. Sea-bed mixing and particle residence times in biologically and physically dominated estuarine systems: a comparison of lower chesapeake bay and the york river subestuary. Estuarine, Coastal and Shelf Science 46, 777 –95.

Drodt, M., Trautwein, A., König, I., Suess, E., Koch, C., 1997. Mössbauer spectroscopic studies on the iron forms of deep-sea sediments. Physics and Chemistry of Minerals 24, 281–93.

Eberl, D., 2003. User's guide to RockJock – A program for determining quantitative mineralogy from powder X-ray diffraction data. U.S. Geological Survey Open-File Report 2003-78, 47 p. edition.

Friedrichs, C.T., Cartwright, G.M., Dickhudt, P.J., 2008. Quantifying Benthic Exchange of Fine Sediment Via Continuous, Non-Invasive Measurements of Settling Velocity and Bed Erodibility. Oceanography 21, 168–72.

Gerringa, L.J.A., 1990. Aerobic degradation of organic matter and the mobility of Cu, Cd, Ni, Pb, Zn, Fe and Mn in marine sediment slurries. Marine Chemistry 29, 355 –74.

Goldberg, E.D., Hodge, V., Koide, M., Griffin, J., Gamble, E., Bricker, O.P., Matisoff, G., Jr., G.R.H., Braun, R., 1978. A pollution history of chesapeake bay. Geochimica et Cosmochimica Acta 42, 1413 –25.

Hedges, J., Keil, R., 1995. Sedimentary organic matter preservation: an assessment and speculative synthesis. Marine Chemistry 49, 81–115.

Horowitz, A.J., Elrick, K.A., 1987. The relation of stream sediment surface area, grain size and composition to trace element chemistry. Applied Geochemistry 2, 437 –51.

Kïg, I., Drodt, M., Suess, E., Trautwein, A., 1997. Iron reduction through the tan-green color transition in deep-sea sediments. Geochimica et Cosmochimica Acta 61, 1679 –83.

König, I., Haeckel, M., Drodt, M., Suess, E., Trautwein, A.X., 1999. Reactive fe(ii) layers in deep-sea sediments. Geochimica et Cosmochimica Acta 63, 1517 –26.

Kostka, J.E., Luther III, G.W., 1994. Partitioning and speciation of solid phase iron in saltmarsh sediments. Geochimica et Cosmochimica Acta 58, 1701–10.

Lagarec, K., Rancourt, D., 1998. Recoil. Mössbauer spectral analysis software for Windows, version 1.

Lewis, D.W., McConchie, D., 1994. Analytical Sedimentology. Chapman and Hall, New York, NY.

Lin, J., Kuo, A., 2001. Secondary turbidity maximum in a partially mixed microtidal estuary. Estuaries and Coasts 24, 707–20.

Long, G., 1984. Mössbauer spectroscopy applied to inorganic chemistry. volume 1. Springer.

Lord III, C., 1980. The chemistry and cycling of iron, manganese and sulfur in salt marsh sediment. PhD thesis. University of Delaware.

McKeague, J., Day, J., 1966. Dithionite- and oxalate-extractable Fe and Al as aids in differentiating various classes of soils. Can. J. Soil Sci , 13–22.

McKee, B.A., Aller, R.C., Allison, M.A., Bianchi, T.S., Kineke, G.C., 2004. Transport and transformation of dissolved and particulate materials on continental margins influenced by major rivers: benthic boundary layer and seabed processes. Continental Shelf Research 24, 899 – 926.

Mehra, O., Jackson, M., 1960. Iron oxide removal from soils and clays by a dithionite–citrate system buffered with sodium bicarbonate, in: 7th Natl. Conf. on Clays and Clay Minerals, pp. 317–27.

Moore, R., Burton, J., Williams, P., Young, M., 1979. The behaviour of dissolved organic material, iron and manganese in estuarine mixing. Geochimica et Cosmochimica Acta 43, 919 –26.

Nichols, M.M., Biggs, R.B., 1985. Estuaries, in: R.A. Davis Jr (Ed.), Coastal Sedimentary Environments. Springer-Verlag, New York, pp. 77–188.

Oh, S., Cook, D., Townsend, H., 1998. Characterization of iron oxides commonly formed as corrosion products on steel. Hyperfine Interactions 112, 59–66. 10.1023/A:1011076308501.

Palomo, L., Canuel, E., 2010. Sources of Fatty Acids in Sediments of the York River Estuary: Relationships with Physical and Biological Processes. Estuaries and Coasts 33, 585–99.

Phillips, E., Lovley, D., 1987. Determination of Fe(III) and Fe(II) in oxalate extracts of sediment. Soil Science Society of America Journal 51, 938–41.

Poulton, S.W., 2003. Sulfide oxidation and iron dissolution kinetics during the reaction of dissolved sulfide with ferrihydrite. Chemical Geology 202, 79–94.

Poulton, S.W., Canfield, D.E., 2005. Development of a sequential extraction procedure for iron: implications for iron partitioning in continentally derived particulates. Chemical Geology 214, 209 –21.

Poulton, S.W., Raiswell, R., 2002. The low-temperature geochemical cycle of iron: From continental fluxes to marine sediment deposition. Am J Sci 302, 774–805.

Poulton, S.W., Raiswell, R., 2005. Chemical and physical characteristics of iron oxides in riverine and glacial meltwater sediments. Chemical Geology 218, 203–21.

Raiswell, R., 2006. Towards a global highly reactive iron cycle. Journal of Geochemical Exploration 88, 436–9.

Raiswell, R., 2011. Iron transport from the continents to the open ocean; the aging-rejuvenation cycle. Elements 7, 101–6.

Raiswell, R., Canfield, D., Berner, R., 1994. A comparison of iron extraction methods for the determination of degree of pyritisation and the recognition of iron-limited pyrite formation. Chemical Geology 111, 101 –10.

Schaffner, L., Dellapenna, T., Hinchey, E., Neubauer, M., Smith, M., Kuehl, S., 2001. Physical energy regimes, seabed dynamics and organism-sediment interactions along an estuarine gradient, in: Aller, J., Woodin, S., Aller, R. (Eds.), Organism-Sediment Interactions. University of South Carolina Press, Columbia, pp. 161–82.

Schwertmann, U., Murad, E., 1990. The influence of aluminum on iron oxides: XIV. Al-substituted magnetite synthesized at ambient temperatures. Clays and Clay Minerals 38, 196–202.

Stookey, L., 1970. Ferrozine—a new spectrophotometric reagent for iron. Analytical Chemistry 42, 779–81.

Sundby, B., Anderson, L., Hall, P., Iverfeldt, Å., van der Loeff, M., Westerlund, S., 1986. The effect of oxygen on release and uptake of cobalt, manganese, iron and phosphate at the sediment-water interface. Geochimica et Cosmochimica Acta 50, 1281 –8.

Takeno, N., 2005. Atlas of Eh-pH Diagrams. Geological Survey of Japan Report no. 419 .

Taylor, K.G., Konhauser, K.O., 2011. Iron in earth surface systems: A major player in chemical and biological processes. Elements 7, 83–8.

Tessier, A., Campbell, P.G.C., Bisson, M., 1979. Sequential extraction procedure for the speciation of particulate trace metals. Analytical Chemistry 51, 844–51.

Virginia Estuarine and Coastal Observing System (VECOS) database, 2007. http://chsd.vims.edu/realtime/. Stations YRK005.4/YRK005.67B (Gloucester Point) and YRK015.09 (Clay Bank). Accessed 12 April 2009.

Walling, C., 1975. Fenton's reagent revisited. Accounts of Chemical Research 8, 125–31.

van der Zee, C., Roberts, D.R., Rancourt, D.G., Slomp, C.P., 2003. Nanogoethite is the dominant reactive oxyhydroxide phase in lake and marine sediments. Geology 31, 993–6.

van der Zee, C., Slomp, C.P., Rancourt, D.G., de Lange, G.J., van Raaphorst, W., 2005. A Mössbauer spectroscopic study of the iron redox transition in eastern Mediterranean sediments. Geochimica et Cosmochimica Acta 69, 441 –53.

VITA

Amy Kathleen Pitts
Department of Ocean and Earth Sciences
Old Dominion University
Norfolk, VA 23529

Education
BA, Biology, May 1999, The University of North Carolina, Chapel Hill, NC

Professional Experience
Contract Specialist, Department of Veterans Affairs, December 2010-present
Procurement Technician, United States Coast Guard, August 2010-December 2010
Educator, Hampton City Schools, February 2004-June 2007
Partner Executive, Clarke American, September 2002-February 2004
Officer, United States Navy, May 1999-September 2002

Presentations
Effect of Physical Reworking and Bioturbation on Sedimentary Reactive Iron within a Microtidal Estuary, Goldschmidt Conference, Knoxville, TN, June 2010
Space School, Virginia Association of Science Teachers Annual Conferenced, Hampton. VA, November 2008
Activities, Materials, and Resources That TEACH SCIENCE!, National Science Teachers' Association Annual Conference, St. Louis, MO, March 2007

Typeset using LaTeX.